Journal of Earth Science, *Vol. 29*, *No. 4*, *p. 920–938*, *August 2018* *ISSN 1674-487X*
Printed in China
https://doi.org/10.1007/s12583-018-0788-2

U-Pb Geochronology, Elemental and Sr-Nd Isotopic Geochemistry of the Houyaoyu Granite Porphyries: Implication for the Genesis of Early Cretaceous Felsic Intrusions in East Qinling

Xiaohu He[1], Hong Zhong*[2,3], Zhifang Zhao[1], Shucheng Tan[1], Weiguang Zhu[2], Siqi Yang[4], Wenjun Hu[2], Zhong Tang[5], Congfa Bao[5]

1. *Department of Geology*, *School of Resource Environment and Earth Science*, *Yunnan University*, *Kunming* 650091, *China*
2. *State Key Laboratory of Ore Deposit Geochemistry*, *Institute of Geochemistry*, *Chinese Academy of Sciences*, *Guiyang* 550081, *China*
3. *University of Chinese Academy of Sciences*, *Beijing* 100049, *China*
4. *Kunming University of Science and Technology*, *Kunming* 650093, *China*
5. *Institute of Yunnan Geology Survey*, *Kunming* 650051, *China*

Xiaohu He: https://orcid.org/0000-0003-0515-3172; Hong Zhong: https://orcid.org/0000-0002-5871-2380

ABSTRACT: The Early Cretaceous Houyaoyu granite porphyries are located in the south margin of the North China Craton. Field observations, petrography, geochronology, major and trace elemental and Sr-Nd isotopic compositions are reported to elucidate the genesis of the Houyaoyu granite porphyries. SIMS zircon U-Pb analyses for the Houyaoyu granite porphyries yield two concordant ages of 133.2±2.3 (2σ) and 131±1.1 (2σ) Ma, respectively. Major and trace elemental compositions indicate that these porphyries are high-K I-type granites with high contents of SiO_2, K_2O, Rb, U, Pb, low Nb, Ta, Ti, and P. Initial $^{87}Sr/^{86}Sr$ ratios range from 0.708 3 to 0.709 7, and $\varepsilon_{Nd}(t)$ values range from -9.13 to -12.3, with corresponding two-stage depleted-mantle Nd model ages (T_{2DM}) varying from 1.57 to 1.91 Ga. This suggests that the Houyaoyu granite porphyries were predominantly derived from ancient lower continental crust, with minor involvement of mantle-derived components. On the basis of the tectonic evolution of the Qinling Orogen and geochemical characteristics of the Houyaoyu granite porphyries, it is proposed that they were formed in an extensional tectonic setting related to lithospheric destruction of the North China Craton, and produced Mo and Pb-Zn mineralization in East Qinling Orogen.

KEY WORDS: East Qinling, granite porphyries, ancient lower continental crust, destruction of North China Craton.

0 INTRODUCTION

The Qinling Orogen is well known as a product of the continent-continent collision between the North China Craton (NCC) and the South China Block (SCB) (Xu and Zhang, 2018; Dong et al., 2012). In the East Qinling, numerous Late Mesozoic igneous rocks (ca. 158–108 Ma) are closely related to molybdenum and Pb-Zn mineralization. Therefore, elucidating the genesis of these intrusions could provide crucial constraints on the formation of the Mo metallogenic belt and Pb-Zn deposits (Zhang Z W et al., 2011, 2007, 2001), such as the Jinduicheng Mo Deposit (mineralization age at 141 Ma, Li H Y et al., 2012), Shiyaogou Mo Deposit (mineralization age at 131 Ma, Gao et al., 2010), Yinjiagou Ag-Pb-Zn Deposit (mineralization age at 143 Ma, Wu and Zheng., 2013a, b). Late Mesozoic intrusions in East Qinling also provide a window on the evolution of the south continental margin of the NCC. Numerous studies on the petrology, geochronology and geochemistry of these intrusions (Fig. 1) have previously been conducted to reveal their genesis (Zeng et al., 2013a, b; Li N et al., 2012; Qi et al., 2012; Xiao et al., 2012; Hu et al., 2011; Mao et al., 2011, 2010; Wang et al., 2011; Gao et al., 2010; Dai et al., 2009; Guo et al., 2009; Ye et al., 2008a; Chen et al., 2003), but a debate about the genesis of these intrusions continues. For example, Zhao et al. (2012) suggested that the intrusions originated from partial melting of the mafic lower continental crust via heating from underlying basaltic melts. Zeng et al. (2013a, b) studied the Babaoshan granitic porphyries adjacent to the Houyaoyu intrusions, and proposed that they were the products of partial melting of the SCB continental crust subducted under the NCC. Chen et al. (2000) and Li N et al. (2007) suggested the intrusions formed from the re-melting of continental crust in a continent-continent

*Corresponding author: zhonghong@vip.gyig.ac.cn

Manuscript received March 3, 2018.
Manuscript accepted June 7, 2018.

He, X. H., Zhong, H., Zhao, Z. F., et al., 2018. U-Pb Geochronology, Elemental and Sr-Nd Isotopic Geochemistry of the Houyaoyu Granite Porphyries: Implication for the Genesis of Early Cretaceous Felsic Intrusions in East Qinling. *Journal of Earth Science*, 29(4): 920–938. https://doi.org/10.1007/s12583-018-0788-2. http://en.earth-science.net

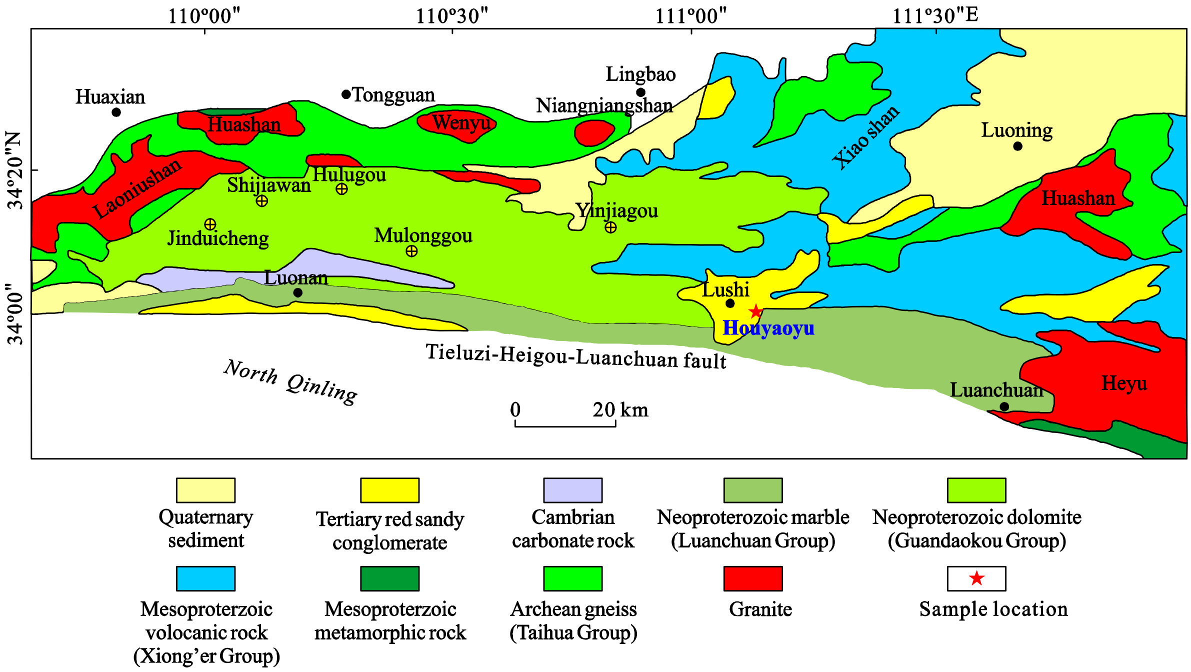

Figure 1. Regional geological map showing the study area within East Qinling orogenic belt (revised after Mao et al., 2010).

collisional setting. In fact, most researchers have suggested that these intrusions were the products of crust-mantle interaction, and that they were mainly derived from the ancient lower continental crust of the NCC involved with a small portion of mantle materials (Zeng et al., 2013a, b; Li N et al., 2012; Qi et al., 2012; Hu et al., 2011; Mao et al., 2011, 2010; Wang et al., 2011; Gao et al., 2010; Dai et al., 2009; Guo et al., 2009; Ye et al., 2008a).

However, the mixing proportions of crust and mantle are still unknown. Previous studies have shown that these small intrusions were formed between ~158 and ~108 Ma, which corresponds to Late Jurassic–Early Cretaceous magmatic activity (Gao et al., 2014; Li N et al., 2012; Hu et al., 2011; Ding et al., 2010; Mao et al., 2010), and during this period the tectonic mechanism of the southern NCC margin was transformed from compression to extension (Xu et al., 2013; Zhai et al., 2004, 2003). Mao et al. (2010) declareed that intensive magmatism was resulted from a lithospheric thinning processes, which may have been induced by either thermal erosion and metasomatism of the subcontinental lithospheric mantle beneath eastern China (Griffin et al., 1998; Menzies and Xu, 1998), or by lithospheric delamination (Deng et al., 2007, 2004; Wu et al., 2005; Gao et al., 2004, 2002).

In this paper, the Houyaoyu granite porphyries in East Qinling are examined on the basis of geochronology, major-trace elemental and Sr-Nd isotopic compositions. It is suggested that the parental magma of the Houyaoyu granite porphyries was mostly derived from partial melting of an over-thickened lower continental crust that was induced by the transformation of the structural system from extrusion to extension together with the involvement of a small amount of mantle material. This study also reveals the discovery of enclaves existing in the Houyaoyu granite porphyries. Based on Sr-Nd isotopic compositions, these enclaves are considered to be representative of the lower NCC crust, which dominantly generated the granitic porphyries. Thus, the present study probably provides common petrogenetic evidence for the magmatic intrusions that formed during the Early Cretaceous in East Qinling.

1 GEOLOGICAL SETTING

The Qinling Orogen is a complex orogenic belt, which recorded the development of plate tectonics from oceanic subduction and arc-type magmatism to arc-continent and continent-continent collision and witnessed major episodes of accretion and collision between discrete continental blocks, such as the NCC, North Qinling Block and the SCB (Chen et al., 2018; Dong and Santosh, 2016; Wu and Zheng, 2013a, b). According to available geology, geochemistry and geochronology materials, Dong and Santosh (2016) suggested that the tectonic history of the Qinling Orogen at least has gone through five stages: (1) The southward subduction of Mesoproterozoic ocean between the North Qinling terrane and NCC led to the collage of the North Qinling terrane and the NCC at ca. 1.0 Ga and remained the Kuanping suture. (2) The Neoproterozoic accretion as represented by the widely distributed terranes and volcanic-sedimentary rocks. (3) Paleozoic two-stage subduction including Early Paleozoic ocean-continent subduction constrained by the ophiolitic mélange, island-arc related volcanics, intrusions and (ultra)high-pressure and (ultra)high-temperature metamorphic events in the North Qinling belt, and Late Paleozoic continent-continent subduction (Bader et al., 2013; Wu and Zheng, 2013a, b; Dong et al., 2011; Meng and Zhang, 2000). (4) The Triassic collisional orogeny occurred between the South Qinling Block and SCB along the Mianlue suture (Wang et al., 2018; Dong et al., 2011; Meng and Zhang, 2000). (5) Mesozoic intra-continental orogeny, including Early Jurassic differential tectonics, Late Jurassic to Early Cretaceous compression and thrusting, and Late Cretaceous to Paleogene orogen collapse and depression (Li N et al., 2015b; Li Y F et al., 2004).

The Houyaoyu granite porphyries are located in the East Qinling Orogen, and belong to part of the southern NCC margin (Fig. 1). The exposed strata are mainly composed of the Upper Taihua Group formed in earlier Paleoproterozoic (medium- to high-grade metamorphic rocks including hornblende schist, amphibolite gneiss) (Li N et al., 2015b; Lu et al., 2015; Xu et al., 2009; Diwu et al., 2007; Chen and Zhao, 1997; Hu et al., 1988), Middle Proterozoic Xiong'er Group (mainly consisting of mafic-intermediate-acid volcanic lava and fluvial to lacustrine facies sedimentary rocks), the Neoproterozoic Guandaokou Group (mainly consisting of carbonate sedimentary formation composed of dolomite), and Quaternary sediments(mainly consisting of loose sand and clay minerals) (Li C Y et al., 2012; Ye et al., 2008a, 2006; Zhang et al., 2011, 1997, 1996). The crystalline basement is the Taihua Group, which consists of intermediate- high grade metamorphic rocks, and the Xiong'er Group, Luanchuan Group, Guandaokou Group, and Quaternary sediments then overlap in this order to form the cover.

Magmatism was fairly frequent and extensive throughout geological history in the East Qinling district, particularly during the Yanshanian Stage. Numerous small intrusions with ages from ~158 to ~108 Ma are exposed (Mao et al., 2010) in this area, which are mainly composed of syenite granite porphyry, (biotite) monzonite granite porphyry, quartz diorite, K-feldspar granite porphyry (Qi et al., 2012; Hu et al., 2011; Wang et al., 2011; Gao et al., 2010; Mao et al., 2010; Dai et al., 2009; Guo et al., 2009; Ye et al., 2008b; Zhang et al., 2006). These small intrusions supplied plenty of ore-forming materials for Mo (W) and Pb-Zn polymetallic mineralization during the Yanshanian Stage, and generated a large-scale molybdenum belt and Pb-Zn polymetallic deposits in eastern Qinling. Furthermore, small amounts of mafic rocks are exposed in this area in the form of batholiths, dikes, veins, and branches (Lu, 1998).

The Houyaoyu granite porphyries were emplaced into the Longjiayuan Formation of the Late Proterozoic Guandaokou Group consisting of dolomite (Fig. 2). The Fe-Pb-Zn ore bodies are located in the contact belt between country rocks and the intrusions, and there are clear boundaries between the intrusions and the Fe-Pb-Zn ore bodies (Fig. 3). Thus, the emplacement of the Houyaoyu granite porphyries is considered to cause the formation of the Houyaoyu Fe-Pb-Zn Deposit.

2 SAMPLES AND ANALYTICAL METHODS

2.1 Samples

Thirteen rock samples with moderate alteration were collected from different areas of the Houyaoyu granite porphyries, and two enclaves (YY-22, YY-56) in the granite intrusion (see Figs. 3e, 3f) were collected. The Houyaoyu granite porphyries and enclaves exhibit massive structures, and porphyritic textures in hand specimen. These samples were systematically identified via microscope and classic porphyritic textures were identified. The Houyaoyu granite porphyries are composed of quartz (20 vol.%–25 vol.%, often showing round and harbor shape by alteration), K-feldspar (40 vol.%–45 vol.%, often exhibiting kaolinization or argillization), biotite (15 vol.%, often exhibiting chloritization), and other minor silicate minerals (e.g., apatite, sphene) and opaque minerals (e.g., pyrite, magnetite). The phenocrysts consist of quartz, K-feldspar and biotite (Figs. 4c, 4d). The two enclaves are significantly different from the Houyaoyu granite porphyries, because they consist of plagioclase with kaolinization, quartz, and show more severe alteration (Figs. 4e, 4f).

To determine the emplacement age of the Houyaoyu granite porphyries, we collected two samples (YY-02 and YY-52) and performed SIMS U-Pb dating on zircons. The petrological characteristics of the two samples are described as follows.

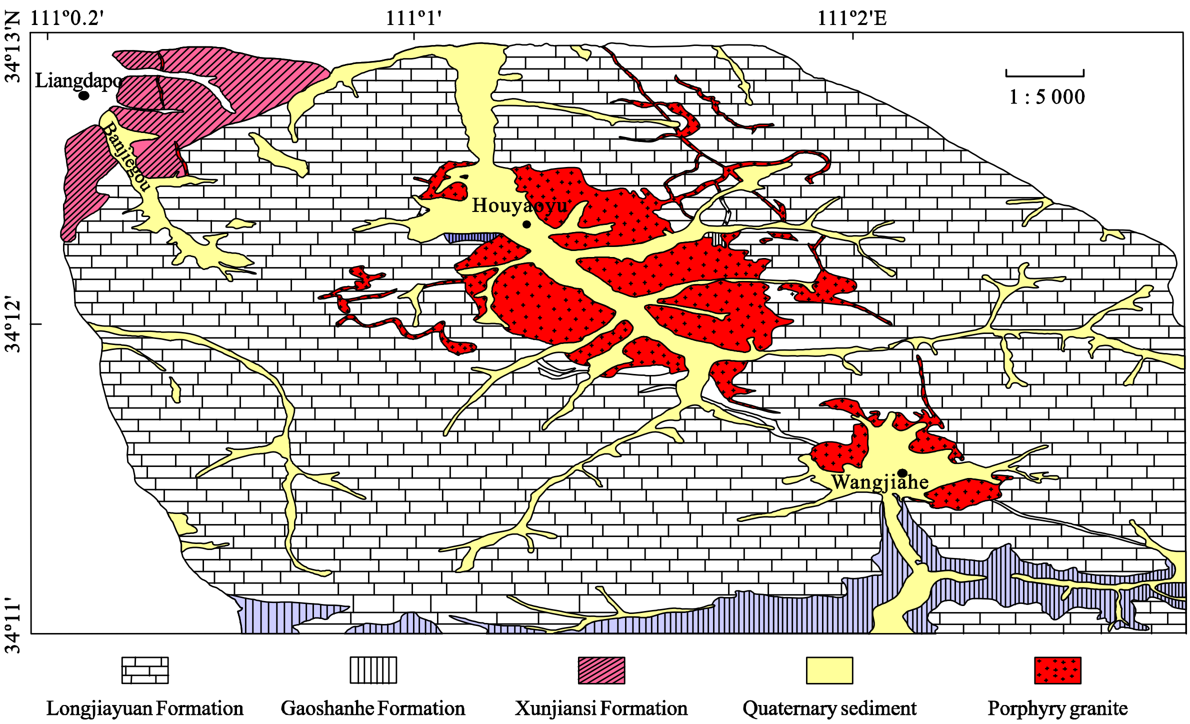

Figure 2. Simplified geological map of the Houyaoyu region.

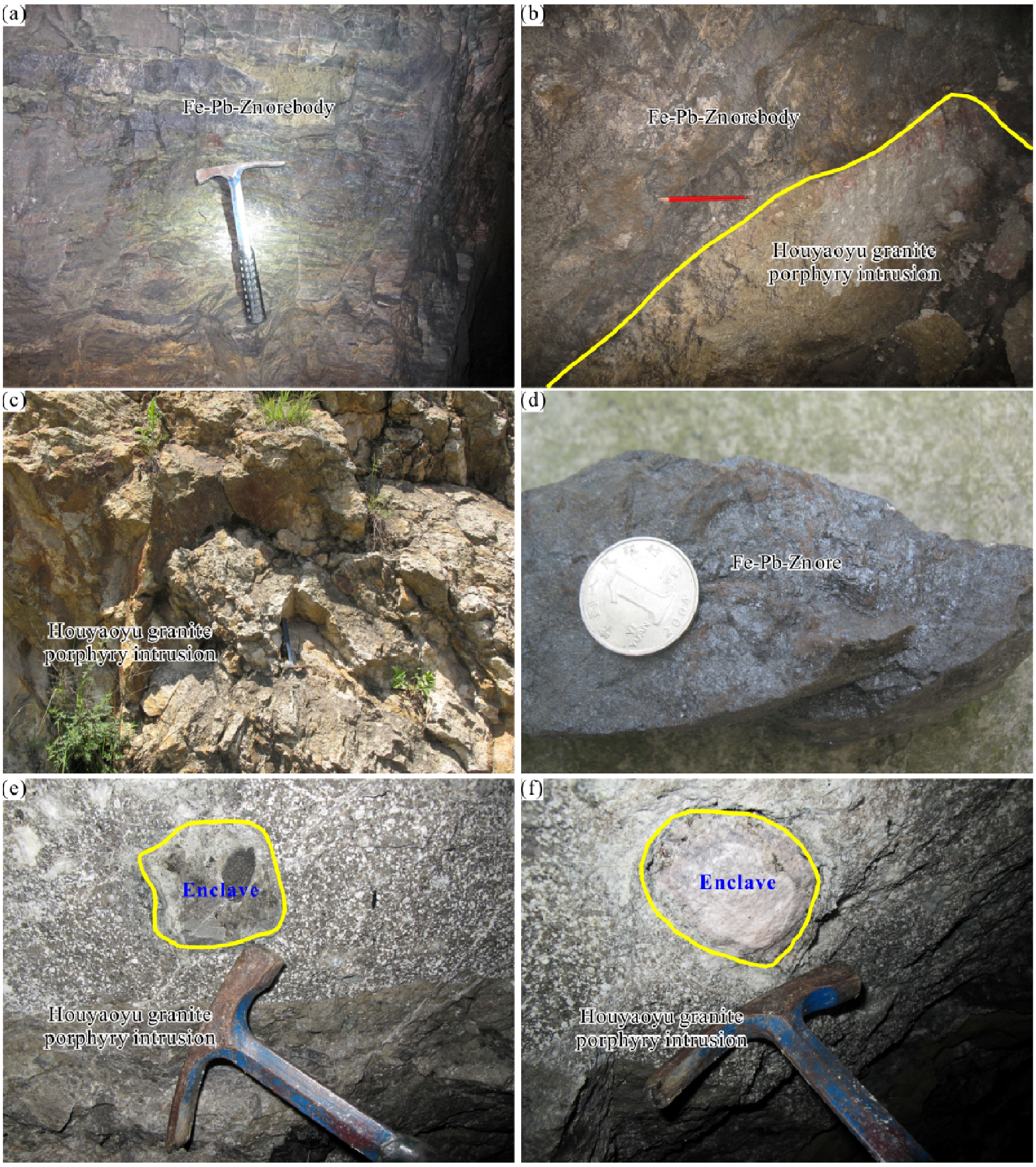

Figure 3. Field photographs of the Houyaoyu granite porphyries and Fe-Pb-Zn ore bodies. (a) Fe-Pb-Zn ore bodies in tunnel; (b) the contact relation between intrusion and ore bodies; (c) the field outcrop of granite; (d) hand specimen of ore; (e) and (f) enclaves in porphyry granite.

Both YY-02 and YY-52 are slightly altered K-feldspar granitic porphyries with porphyritic textures and matrixes consisting of K-feldspar, plagioclase, quartz, and biotite, as well as accessory minerals including zircon, apatite, and iron-titanium oxides. The phenocrysts mainly comprises of quartz, altered K-feldspar, and biotite (Fig. 4). As no zircon grains were obtained from the enclaves, we are unable to determine the age of the enclaves.

2.2 Geochronology

Two samples (YY-02 and YY-52) were firstly grounded into powder. The zircons were separated using heavy liquid method before being handpicked out under a binocular microscope for mounting in epoxy resin. To identify the internal structure and choose potential target sites for the U-Pb analysis of zircon, cathodeluminescence (CL) images were obtained (Fig. 5) using a scanning electron microanalyzer at the Institute of Geology and Geophysics, Chinese Academy of Sciences (IGGCAS), Beijing.

Measurements of U, Th, and Pb isotopes were conducted using the Cameca IMS-1280 secondary ion mass spectrometer (SIMS) at the IGGCAS. U-Th-Pb ratios and absolute abundances were determined according to standard zircon 91500 (Wiedenbeck et al., 1995). The detailed analytical methods are described in Li X H et al. (2009). A long-term uncertainty of 1.5% (1 RSD) for $^{206}Pb/^{238}U$ measurements of standard zircons was propagated to the unknown zircons (Li et al., 2010; Sláma et al., 2008; Black et al., 2004), even though the measured $^{206}Pb/^{238}U$ error in a specific session was generally around 1% (1 RSD) or less. Measured compositions were corrected for common Pb using non-radiogenic ^{204}Pb, but corrections were found to be sufficiently small to be insensitive to the choice of common Pb composition, and an average of present-day crustal composition (Stacey and Kramers, 1975) was used for common Pb (assuming that common Pb is largely related to surface contamination introduced during sample preparation). Uncertainties related to individual analysis are reported at 1σ level, and mean ages for pooled U/Pb (and Pb/Pb) analyses are quoted with a 95% confidence interval. Data reduction was conducted using the Isoplot/Ex v. 2.49 program (Ludwig, 2001).

2.3 Major and Trace Element

All of the studied rock samples were collected from the Houyaoyu granite porphyries. Major oxides of the samples were measured using an Axios PW4400 X-ray fluorescence spectrometer (XRF) on fused glass beads at ALS Chemex (Guangzhou) Co. Ltd, and trace elements were analyzed using inductively coupled plasma mass spectrometry (ICP-MS) at the State Key Laboratory of Ore Deposit Geochemistry (SKLODG), Chinese Academy of Sciences (CAS), following the procedures of Qi et al. (2000). Instrumental drift was corrected running a reference standard solution after every five samples. Results show that analytical precisions and accuracies for most of the trace elements measured were generally better than 5%.

2.4 Sr-Nd Isotope

The chemical separation and isotopic measurement procedures were described in Zhang G W et al. (2001).Whole-rock Sr-Nd isotopic analyses were performed using a VG AXIOM multi collector-ICP-MS (MC-ICP-MS) at the Key Laboratory of Orogenic Belts and Crustal Evolution, Ministry of Education, Peking University.

Mass fractionation corrections for Sr and Nd isotopic ratios were based on the $^{86}Sr/^{88}Sr$ ratio of 0.119 4 and $^{146}Nd/^{144}Nd$ ratio of 0.721 9, respectively. The $^{87}Sr/^{86}Sr$ ratio of the Standard NBS987 and $^{143}Nd/^{144}Nd$ ratio of the Standard SHINESTU

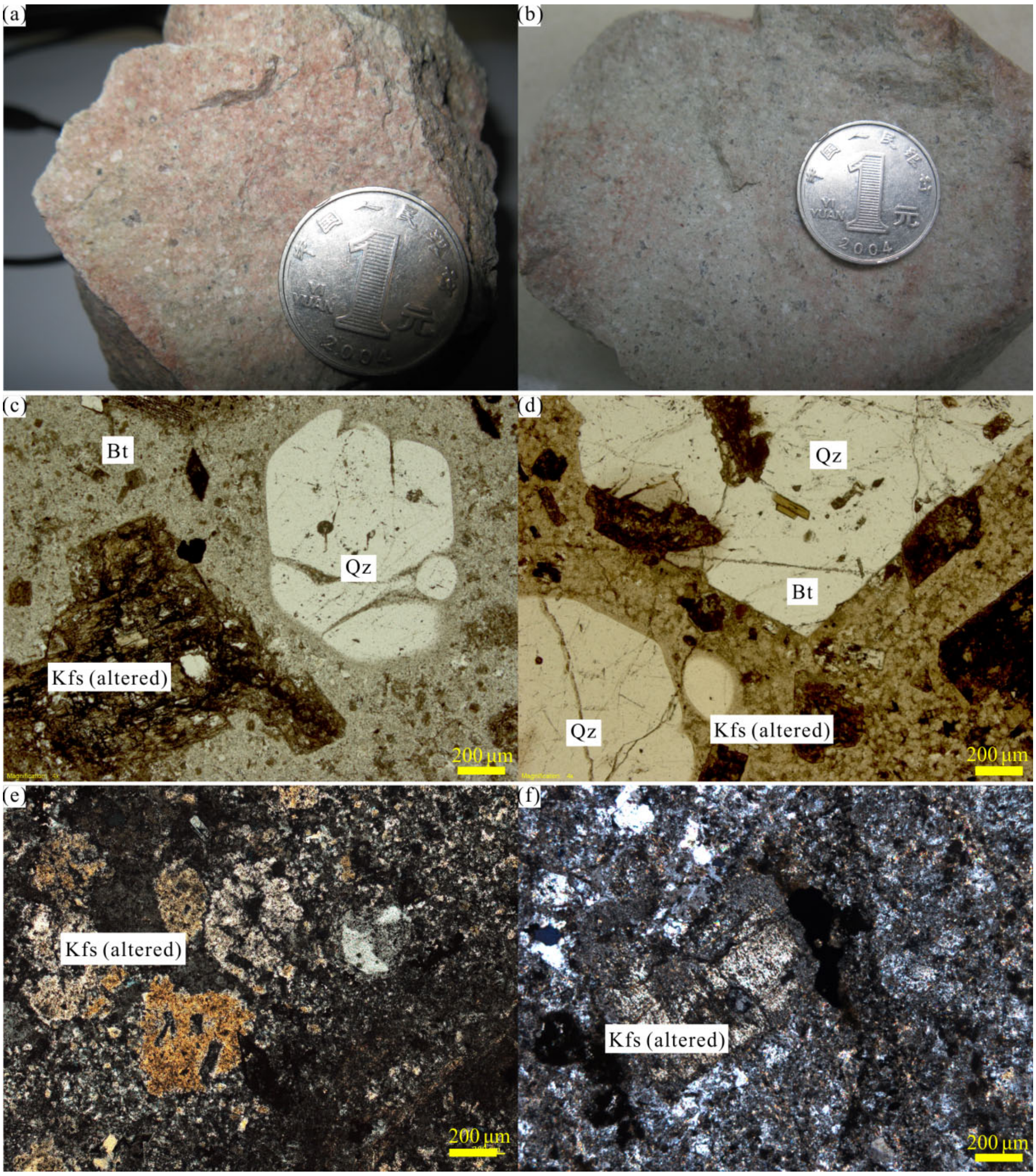

Figure 4. Hand specimen and microscope photos of the Houyaoyu granite porphyries. (a), (b) are hand specimen showing that they are massive structure and porphyritic texture; (c), (d) are photomicrograph showing that the Houyaoyu granite porphyries with classic porphyritic texture consist of quartz (Qz), K-feldspar (Kfs), biotite (Bt), apatite, sphene, pyrite (Py), magnetite. Furthermore, phenocrysts consist of quartz, K-feldspar and biotite, and the same is true for matrix composition; (e), (f) are photomicrograph from YY-22 and YY-56.

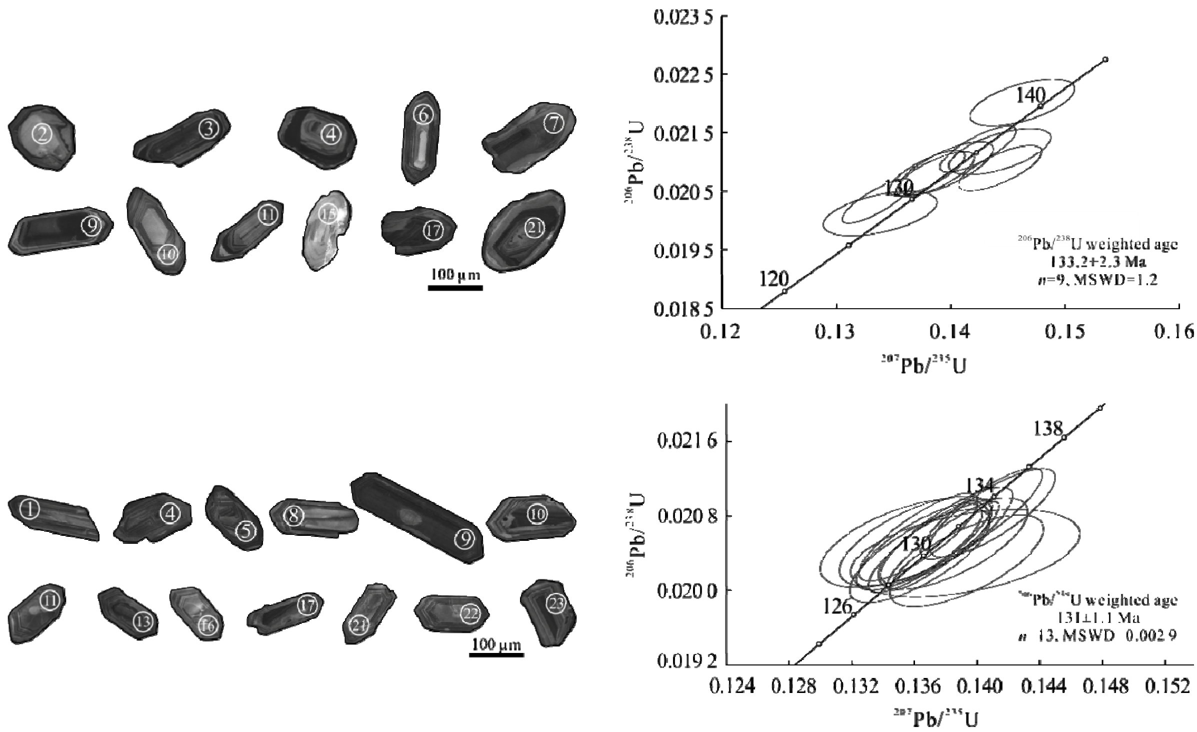

Figure 5. Representative cathodoluminescene (CL) images SIMS zircon U-Pb concordia diagram of selected zircons from the Houyaoyu granite porphyries.

determined in this study were 0.710 250±0.000 007 (2σ) and 0.512 118±0.000 003 (2σ), respectively.

3 RESULTS

3.1 Zircon U-Pb Geochronology

In the CL images, all zircon grains show typical oscillatory zoning (Fig. 5), which are typical characteristics of magmatic zircon. Most of the Th/U ratios range between 0.2 and 1.17 (Table 1), greater than 0.1, it suggests a magmatic origin (Wu and Zheng, 2004; Belousova et al., 2002). The crystals from YY-02 and YY-52 are brown and translucent in relation to radioactive damage from their high-uranium contents (Li N et al., 2007).

All U-Pb data for the zircons of two samples collected from the Houyaoyu granite porphyries are presented in Table 1. Based on 9 and 13 analytical results of YY-02 and YY-52, respectively, two weighted mean average ^{206}Pb/^{238}U ages of 133.2±2.3 Ma (2σ, MSWD=1.2) and 131±1.1 Ma (2σ, MSWD=0.002 9) were obtained for the Houyaoyu granite porphyries (Fig. 5). In addition, four older ^{207}Pb/^{206}U ages (1 791.7±10.6, 1 925.5±7.4, 2 500.8±5.8, 2 498.5±5.1 Ma) were obtained for Sample YY-02, which are representative of the ages of inherited zircon grains from ancient strata of the NCC.

3.2 Major and Trace Element Geochemistry

Major and trace elemental data of 15 samples for the Houyaoyu granite porphyries are listed in Table 2. Most of the rock samples had been subjected to moderate alteration and had high LOI values ranging from 2.27 wt.% to 7.33 wt.% (mostly between 2.27 wt.% and 4.11 wt.%). Their major oxide contents (recalculated to 100 wt.% in a volatile-free as discussed below) were slightly variable, with SiO_2 contents ranging from 68.28 wt.% to 74.06 wt.%, Al_2O_3 from 12.89 wt.% to 15.97 wt.%, MgO from 0.21 wt.% to 1.66 wt.%, CaO from 0.39 wt.% to 3.26 wt.%, and Fe_2O_3 from 0.86 wt.% to 3.55 wt.%, respectively. In the TAS diagram, most samples are plotted in the granite area and only a few are plotted into the granodiorite and quartz monzonite area (Fig. 6a). In addition, most samples are plotted into the high-K area in the K_2O-SiO_2 diagram (Fig. 6b). It is considered that the relatively high Na_2O+K_2O values (3.58 wt.%–7.34 wt.%) and the highly variable K_2O/Na_2O ratios (1.43–24.46) could result from late alteration, which would produce a moderate degree of deviation in the K_2O-SiO_2 and TAS diagrams. The Rittmann indexes (σ) ranged between 0.46 and 2.59 (average 2.0), indicating that these rocks belong to the shoshonitic and high-K alkaline series.

Although the trace element contents of the Houyaoyu granite porphyries are largely variable, their primitive mantle-normalized trace element patterns are mostly similar to each other (Fig. 7a), indicating that they could have shared a common parental magma, or were most likely derived from a similar source. They are enriched in LILEs (such as Ba, Th, U, K), Pb, and depleted in Nb, Ta, P and Sr, similar to those of other intrusions formed during the Mesozoic in East Qinling (Li D et al., 2012; Qi et al., 2012; Zhao et al., 2012). The ratios of Nb/Ta, Zr/Hf of all samples are similar, 12.88–18.42 (average 15.74) and 37.89–41.04 (average 39.46), respectively. Some of the geochemical characteristics of these granites are similar to those of the adakites defined by Defant and Drummond (1990), with respect to be depleted in Y (<18 ppm) and Yb (<1.9 ppm), and enriched in Sr (rarely <400 ppm) with high Sr/Y and La/Yb ratios. They are also characterized by strong LREE enrichment on the chondrite-normalized REE diagram, with $(La/Yb)_N$ values varying from 40 to 82, and δEu varying from 0.69 to 0.98 (Table 2).

However, the two enclaves (YY-22, YY-56) have obviously different geochemical characteristics, showing higher

Table 1 Cameca SIMS zircon U-Pb isotopic compositions of samples YY-02 and YY-52 from the Houyaoyu granite porphyries

Sample No.	U	Th	Th/U	$^{206}Pb/^{204}Pb$	Isotopic ratio						Age (Ma)					
	ppm	ppm		measured	$^{207}Pb/^{206}Pb$	±1σ (%)	$^{207}Pb/^{235}U$	±1σ (%)	$^{206}Pb/^{238}U$	±1σ (%)	$^{207}Pb/^{235}U$	±1σ (%)	$^{206}Pb/^{238}U$	±1σ (%)	$^{207}Pb/^{206}Pb$	±1σ (%)
YY-02																
2	131	64	0.487	30 737	0.109 53	0.59	4.730 28	1.61	0.313 2	1.50	1 772.6	13.6	1 756.5	23.1	1 791.7	10.6
3	659	275	0.417	83 141	0.164 34	0.35	10.449 53	1.55	0.461 2	1.52	2 475.5	14.5	2 444.7	30.9	2 500.8	5.8
4	301	211	0.700	48 764	0.164 12	0.31	10.224 04	1.59	0.451 8	1.57	2 455.3	14.9	2 403.4	31.5	2 498.5	5.1
6	563	411	0.729	5 205	0.050 10	1.41	0.144 31	2.06	0.020 9	1.50	136.9	2.6	133.3	2.0	199.5	32.4
7	555	143	0.257	11 117	0.049 42	2.00	0.144 29	2.51	0.021 2	1.52	136.9	3.2	135.1	2.0	167.9	46.0
9	1 489	554	0.372	6 571	0.048 35	1.36	0.138 64	2.02	0.020 8	1.50	131.8	2.5	132.7	2.0	116.6	31.6
10	1 394	280	0.201	5 946	0.048 06	1.27	0.137 90	1.97	0.020 8	1.51	131.2	2.4	132.8	2.0	102.1	29.8
11	221	109	0.494	5 225	0.048 22	2.63	0.133 79	3.05	0.020 1	1.54	127.5	3.7	128.4	2.0	110.1	61.0
15	1 409	11	0.008	21 702	0.048 67	1.16	0.142 39	1.90	0.021 2	1.51	135.2	2.4	135.3	2.0	132.1	27.1
17	1 041	243	0.233	19 575	0.047 62	1.08	0.133 50	1.86	0.020 3	1.52	127.2	2.2	129.8	1.9	80.4	25.4
19	930	339	0.364	39 952	0.117 96	0.41	4.999 39	1.56	0.307 4	1.50	1 819.2	13.2	1 727.8	22.8	1 925.5	7.4
21	453	219	0.483	7 190	0.048 18	2.07	0.146 24	2.56	0.022 0	1.50	138.6	3.3	140.4	2.1	108.2	48.3
YY-52																
1	753	884	1.175	30 651	0.048 31	1.23	0.136 32	1.94	0.020 5	1.50	129.8	2.4	130.6	1.9	114.3	28.8
4	884	325	0.367	18 087	0.048 99	1.63	0.138 49	2.28	0.020 5	1.59	131.7	2.8	130.8	2.1	147.4	37.9
5	1 198	220	0.184	31 329	0.049 08	1.14	0.140 98	1.89	0.020 8	1.50	133.9	2.4	132.9	2.0	151.8	26.5
8	978	442	0.452	10 935	0.048 63	1.15	0.138 06	2.01	0.020 6	1.65	131.3	2.5	131.4	2.1	129.9	26.7
9	2 736	671	0.245	11 651	0.048 82	0.75	0.137 84	1.71	0.020 5	1.54	131.1	2.1	130.7	2.0	139.2	17.6
10	2 173	603	0.277	5 283	0.048 87	0.97	0.140 29	1.83	0.020 8	1.55	133.3	2.3	132.8	2.0	141.4	22.6
11	1 193	814	0.682	20 468	0.048 52	0.99	0.137 01	1.90	0.020 5	1.62	130.4	2.3	130.7	2.1	124.7	23.3
13	1 747	771	0.442	1 088	0.047 89	2.15	0.135 41	2.64	0.020 5	1.54	128.9	3.2	130.9	2.0	93.6	50.1
16	2 097	1 337	0.637	1 339	0.049 51	3.12	0.139 26	3.47	0.020 4	1.51	132.4	4.3	130.2	1.9	171.9	71.3
17	1 025	619	0.603	2 977	0.048 08	1.78	0.136 08	2.36	0.020 5	1.55	129.5	2.9	131.0	2.0	103.0	41.4
21	762	266	0.349	10 101	0.048 55	1.45	0.136 35	2.17	0.020 4	1.62	129.8	2.6	130.0	2.1	125.9	33.7
22	532	206	0.388	6 299	0.049 73	1.69	0.139 35	2.33	0.020 3	1.60	132.5	2.9	129.7	2.1	182.6	38.8
23	1 834	485	0.264	4 881	0.048 05	1.05	0.136 26	1.84	0.020 6	1.51	129.7	2.2	131.2	2.0	101.6	24.7

Table 2 Major (wt.%) and trace element (ppm) compositions of the Houyaoyu granite porphyries and enclaves

Sample No.	WJH-01	YY-02	WJH-03	YY-01	YY-31	YY-32	YY-34	YY-40	YY-45	YY-48	YY-49	YY-52	YY-61	YY-22	YY-56
Rock type	Granite porphyry													Enclave	
SiO_2	66.40	66.10	66.90	65.70	69.90	70.20	67.10	69.40	71.40	68.70	67.50	72.20	69.20	64.30	60.20
Al_2O_3	14.70	15.10	14.80	14.35	13.30	14.30	14.80	14.25	12.55	15.60	14.95	12.80	14.25	13.75	11.25
Fe_2O_3	2.17	2.64	2.09	2.26	1.05	0.84	3.40	2.56	1.96	3.03	2.11	1.22	0.89	1.90	3.75
CaO	3.00	2.54	3.14	3.02	1.80	1.86	1.70	0.84	0.99	0.38	2.36	0.84	2.10	2.16	5.90
MgO	0.48	0.67	0.31	1.54	1.43	0.98	1.10	0.87	0.70	0.21	0.42	1.08	1.16	1.34	1.83
Na_2O	3.05	3.21	2.88	0.13	0.49	2.18	1.46	0.93	0.78	2.49	2.22	0.64	2.49	0.44	0.54
K_2O	4.37	4.62	4.37	3.18	7.29	5.94	4.78	6.92	6.86	5.19	4.95	6.53	4.8	9.73	5.89
TiO_2	0.35	0.35	0.34	0.35	0.34	0.33	0.37	0.37	0.32	0.38	0.36	0.30	0.33	0.87	0.69
MnO	0.13	0.08	0.10	0.22	0.09	0.08	0.06	0.04	0.05	0.09	0.08	0.05	0.07	0.09	0.20
P_2O_5	0.16	0.16	0.16	0.16	0.14	0.13	0.18	0.15	0.14	0.17	0.17	0.12	0.13	0.30	0.18
LOI	3.65	3.19	3.68	7.33	3.73	2.62	4.11	2.89	2.64	2.27	3.63	2.51	3.29	3.24	7.77
Total	98.94	99.54	99.09	98.87	100.9	99.87	99.77	99.63	98.97	98.96	99.21	100.10	99.87	100.60	100.90
A/NK	1.51	1.47	1.56	3.93	1.53	1.43	1.95	1.58	1.44	1.61	1.66	1.58	1.53	1.35	1.75
A/CNK	0.97	1.01	0.98	1.57	1.11	1.07	1.39	1.35	1.19	1.50	1.12	1.33	1.09	1.12	0.91
K_2O/Na_2O	1.43	1.44	1.52	24.46	14.88	2.72	3.27	7.44	8.79	2.08	2.23	10.20	1.93	22.1	10.9
σ	2.29	2.59	2.14	0.46	2.21	2.39	1.57	2.30	2.03	2.26	2.05	1.74	1.99	4.86	2.40
Sc	2.60	2.60	2.61	3.17	3.65	2.74	3.00	3.64	2.95	2.40	2.39	2.61	2.70	11.8	8.88
V	27.4	29.9	31.2	27.6	33.7	26.3	31.6	32.6	40.2	30.1	28.5	22.4	24.5	40.0	18.7
Cu	3.54	2.32	2.25	2.93	2.19	2.93	2.35	181	154	15.7	2.39	1775	3.15	14.6	17.9
Zn	175	111	99.5	1065	29.6	49.4	80.8	354	123	381	194	57.4	94.5	53.6	257
Ga	17.1	17.4	17.2	17.0	17.8	18.9	18.1	22.4	22.4	16.9	16.5	20.1	18.1	14.5	14.2
Rb	136	137	136	122	200	130	138	156	128	141	146	168	113	226	150
Sr	712	704	567	180	100	282	328	159	150	496	511	123	320	53.7	82.7
Y	12.9	12.5	15.7	11.5	10.6	9.64	10.7	7.38	6.09	10.8	11.5	8.28	9.50	18.7	36.4
Zr	226	229	236	223	207	200	222	235	190	234	227	186	199	408	372
Nb	19.1	19.2	19.5	18.3	16.5	16.2	18.1	20.6	16.4	19.7	18.8	17.4	15.6	32.0	17.7

Table 2 Continued

Sample No.	WJH-01	YY-02	WJH-03	YY-01	YY-31	YY-32	YY-34	YY-40	YY-45	YY-48	YY-49	YY-52	YY-61	YY-22	YY-56
Rock type	Granite porphyry													Enclave	
Mo	0.67	0.42	0.54	1.60	2.99	0.88	0.77	4.44	2.66	7.42	1.70	54.8	4.49	11.8	1.71
Ba	1 812	2 021	1 741	1 343	1 121	1 302	1 719	1 060	1 020	2 113	1 860	1 015	1 245	6 450	2 268
La	58.4	57.5	67.3	53.5	50.7	46.6	43.4	25.3	22.0	54.7	56.1	44.4	46.2	10.7	89.9
Ce	97.0	97.5	98.8	91.0	88.1	79.9	79.1	51.5	41.3	95.8	92.5	75.4	77.4	28.5	153.6
Pr	10.6	10.6	11.8	9.83	9.57	8.77	8.88	5.54	4.34	9.91	10.1	7.98	8.41	3.83	18.2
Nd	35.5	35.1	38.7	32.2	31.6	28.7	30.4	21.2	16.2	33.0	33.5	26.4	27.5	16.9	65.4
Sm	5.45	5.43	5.77	5.07	5.08	4.58	4.83	3.48	2.68	5.15	5.16	4.09	4.41	3.45	10.9
Eu	1.59	1.69	1.74	1.33	1.37	1.35	1.45	0.723	0.620	1.60	1.53	1.01	1.26	0.725	2.55
Gd	5.22	4.99	5.41	4.62	4.50	4.18	4.37	2.73	2.35	4.64	4.80	3.58	3.93	3.24	10.4
Tb	0.55	0.56	0.63	0.51	0.48	0.44	0.49	0.36	0.27	0.51	0.52	0.39	0.43	0.485	1.42
Dy	2.44	2.31	2.66	2.19	2.01	1.89	2.11	1.49	1.09	2.14	2.22	1.53	1.77	2.93	6.86
Ho	0.47	0.45	0.51	0.43	0.36	0.33	0.38	0.25	0.20	0.40	0.41	0.28	0.33	0.636	1.46
Er	1.18	1.14	1.35	1.12	0.92	0.90	1.09	0.79	0.64	1.07	1.08	0.69	0.84	2.21	3.98
Tm	0.15	0.15	0.16	0.15	0.12	0.11	0.13	0.09	0.07	0.13	0.13	0.09	0.12	0.362	0.565
Yb	0.98	0.94	1.07	0.90	0.81	0.73	0.88	0.64	0.49	0.85	0.91	0.54	0.74	2.5	3.76
Lu	0.15	0.14	0.15	0.13	0.13	0.11	0.13	0.09	0.08	0.12	0.14	0.09	0.11	0.412	0.582
Hf	5.68	5.75	6.00	5.63	5.22	5.24	5.41	5.88	4.72	5.83	5.82	4.86	5.26	10.1	9.60
Ta	1.04	1.07	1.23	1.14	1.14	1.17	1.19	1.25	1.00	1.21	1.15	1.36	1.09	1.36	1.23
Pb	110	34.5	31.4	257	14.1	48.9	29.3	41.6	26.4	28.8	31.3	38.5	70.8	83.1	95.0
Th	15.3	15.1	15.9	14.5	18.0	18.5	15.0	17.6	15.1	15.6	14.2	15.6	17.7	13.7	17.1
U	2.95	3.82	1.95	3.07	11.28	6.14	3.13	2.30	1.90	3.43	1.54	3.54	5.63	2.47	2.44
Nb/Ta	18.42	18.01	15.87	16.15	14.47	13.83	15.22	16.50	16.40	16.24	16.40	12.77	14.29	23.45	14.37
Zr/Hf	39.83	39.78	39.31	39.63	39.78	38.05	41.04	39.97	40.25	40.15	38.98	38.32	37.89	40.40	38.77
Sr/Ba	0.39	0.35	0.33	0.13	0.09	0.22	0.19	0.15	0.15	0.23	0.27	0.12	0.26	0.008	0.036
Sr/Y	55	57	36	16	9	29	31	22	25	46	45	15	34	2.87	2.27
La/Yb	59	61	63	59	63	63	50	40	45	64	62	82	62	4.28	23.89
δEu	0.90	0.97	0.94	0.82	0.86	0.93	0.95	0.69	0.74	0.98	0.93	0.79	0.91	0.65	0.72

contents of K_2O, MgO, CaO, TiO_2, Y, and lower of Al_2O_3, Sr.

3.3 Sr-Nd Isotopic Compositions

In this study, eight samples from the Houyaoyu granite porphyries were analyzed to obtain their whole-rock Rb, Sr, Sm, Nd concentrations and Sr-Nd isotopic compositions (Table 3). Using results of SIMS zircon U-Pb dating for the Houyaoyu granite porphyries, the initial $^{87}Sr/^{86}Sr$ and $\varepsilon_{Nd}(t)$ values were calculated at t=131 Ma. In addition, depleted mantle Nd model ages (T_{DM}) were calculated using the model of DePaolo (1991). Most of the Sr-Nd isotopic compositions of the Houyaoyu granite porphyries are characterized by relatively homogenous initial $^{87}Sr/^{86}Sr$ ratios ranging from 0.707 7 to 0.709 7, and $\varepsilon_{Nd}(t)$ values ranging from -9.13 to -12.32 (see Table 1 and Fig. 8), with corresponding two-stage depleted-mantle Nd model ages (T_{2DM}) ranging from 1.57 to 1.91 Ga (with the exception of two samples YY-22, YY-56). Notably, two exceptional samples YY-22 and YY-56 have fairly high I_{Sr} (0.734 5 and 0.747 5) and negative $\varepsilon_{Nd}(t)$ values (-24.26 and -26.04).

4 DISCUSSION

4.1 Petrogenesis of the Houyaoyu Granite Porphyries

The results show that major oxides (Fe_2O_3, CaO, Al_2O_3, P_2O_5) and Sr concentrations decrease with increasing values of SiO_2, indicating fractionation of Fe-Ti oxides, plagioclase, and apatite (Fig. 9). It is considered that apatite may have played an important role in parental magmatic evolution, as shown by the obvious depletion of P in the spider diagram (Fig. 7b). In addition, the negative Nb and Ta anomalies (Fig.7a) may be related to the following two occurrences: (1) separation of Ti containing minerals (e.g., titanite and rutile) from magma; (2) parental magma derived from a source depleted in Nb and Ta. However, as the TiO_2 contents show no relationship with the SiO_2 contents (Fig. 6b), this suggests that the Houyaoyu granite porphyries were derived from a crustal source slightly depleted in Nb and Ta.

According to the nature of their protolith, granitic rocks have commonly been divided into I-type, S-type and M-type (Chappell and White, 1974). Loiselle and Wones (1979) later introduced A-type granite, where A stands for mildly alkaline, anorogenic, and anhydrous, according to the chemical compositions. In the Zr vs. TiO_2 diagram (Fig. 10a), the Houyaoyu granite porphyries are plotted into the I-type granite field, and this is also supported by the P_2O_5 vs. SiO_2 diagram (Fig. 9f). It should be noted, however, that due to moderate alternation, the Na_2O contents decrease with increasing SiO_2 (Fig. 6b), thereby causing a distortion of the A/CNK values. Therefore, the A/CNK values cannot be used to distinguish I-type and S-type granite. In contrast, Zr and Ti are immobile elements and were hardly affected by later alteration, thus the Zr vs. TiO_2 diagram is reliable for classification (Hastie et al., 2007). In addition, the P_2O_5 contents slightly decrease with increasing SiO_2 (Fig. 9f), thereby showing a good trend and indicating the characteristics of I-type granite (Li et al., 2007; Chappell and White, 1992). As diagnostic peraluminous minerals such as muscovite, cordierite, and garnet in S-type granites (Barbarin, 1999) were not found in the Houyaoyu granite porphyries, we therefore classify the Houyaoyu granite porphyries as I-type granites.

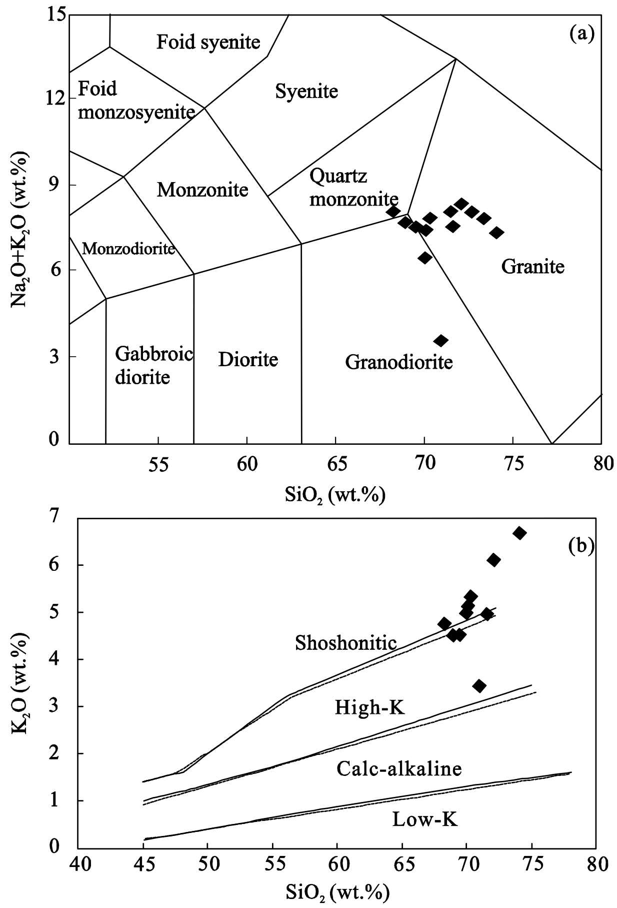

Figure 6. (a) SiO_2 versus total alkali (Na_2O+K_2O) (TAS) (after Middlemost, 1994); (b) K_2O versus SiO_2 diagram of the Houyaoyu granite porphyries (solid line after Peccerillo and Taylor, 1976; dashed line after Middlemost, 1985).

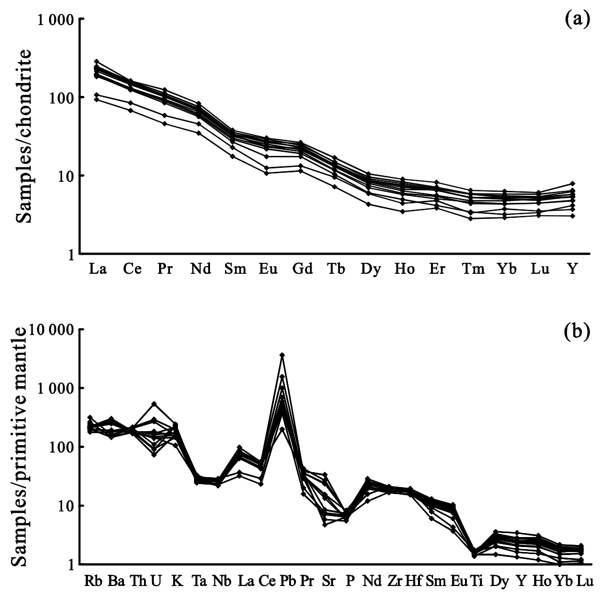

Figure 7. Plots of primitive mantle-normalized incompatible trace-element and chondrite-normalized rare earth element for the Houyaoyu granite porphyries. Primitive mantle data are from Sun and McDonough (1989), and chondrite data from Boynton (1984).

Table 3 Whole-rock Sr-Nd isotopic compositions for the Houyaoyu granite porphyries and enclaves

Sample No.	Rb (ppm)	Sr (ppm)	$^{87}Rb/^{86}Sr$	2σ	$^{87}Sr/^{86}Sr$	I_{Sr}	Sm (ppm)	Nd (ppm)	$^{147}Sm/^{144}Nd$	2σ	$^{143}Nd/^{144}Nd$	$^{143}Nd/^{144}Nd$ (*i*)	$\varepsilon_{Nd}(t)$	T_{DM} (Ma)	T_{2DM} (Ma)
YY-01	136	712	0.553 6	18	0.710 174	0.709 143	5.45	35.53	0.092 7	19	0.511 991	0.511 912	-10.88	1 457	1 792
YY-34	138	328	1.223 7	15	0.710 698	0.708 419	4.83	30.39	0.096 0	18	0.511 920	0.511 838	-12.32	1 589	1 910
YY-40	141	143	2.866 8	18	0.713 013	0.707 675	3.29	19.23	0.103 3	19	0.512 145	0.512 057	-8.05	1 385	1 569
YY-46	145	102	4.114 9	15	0.715 494	0.707 832	1.19	6.57	0.109 8	14	0.512 131	0.512 037	-8.45	1 493	1 604
YY-48	141	496	0.821 0	14	0.709 861	0.708 333	5.15	32.98	0.094 3	14	0.511 932	0.511 851	-12.07	1 553	1 889
YY-52	168	123	3.974 9	17	0.717 068	0.709 667	4.09	26.38	0.093 8	15	0.512 082	0.512 001	-9.13	1 356	1 651
YY-22	235	52	13.226 0	15	0.759 142	0.734 516	3.37	20.02	0.101 6	17	0.511 335	0.511 224	-23.83	2 457	2 844
YY-56	150	83	5.274 0	17	0.757 323	0.747 503	10.90	65.44	0.100 7	18	0.511 221	0.511 135	-26.04	2 588	3 021

Note: $^{87}Rb/^{86}Sr$ and $^{147}Sm/^{144}Nd$ ratios are calculated using Rb, Sr, Sm and Nd contents from Table 2; I_{Sr}=$(^{87}Sr/^{86}Sr)_i$ and $\varepsilon_{Nd}(t)$ values are calculated at *t*=131 Ma; $\varepsilon_{Nd}(t)$ values are calculated using present-day $(^{147}Sm/^{144}Nd)_{CHUR}$=0.196 7 and $(^{143}Nd/^{144}Nd)_{CHUR}$=0.512 638; T_{DM} values are calculated using present-day $(^{147}Sm/^{144}Nd)_{DM}$=0.213 7 and $(^{143}Nd/^{144}Nd)_{DM}$=0.513 15.

Rocks from the Houyaoyu granite porphyries have high Sr (100 ppm–712 ppm, mostly >400 ppm), low Y (6.09 ppm–15.7 ppm, <18 ppm) and Yb (0.493 ppm–1.07 ppm, <1.8 ppm), similar to the geochemical characteristics of adakitic rocks (Castillo, 2012; Richards and Kerrich, 2007; Martin et al., 2005; Defant and Drummond, 1990). Previous studies have revealed that most Late Jurassic–Early Cretaceous granites in East China and in the south of the NCC have characteristics of high Sr and low Y (Li H Y et al., 2012; Li N et al., 2012; Qi et al., 2012; Wang et al., 2011; Gao et al., 2010; Dai et al., 2009; Ye et al., 2008a; Zhang et al., 2006; Zhai, 2004).

Generally, adakitic rocks are formed via the following three mechanisms: (1) partial melting of oceanic slab in a subduction setting (He et al., 2014; Gutscher et al., 2000; Yogodzinski and Kelemen, 1998; Defant and Drummond, 1990); (2) basaltic magmas experiencing complex fractional crystallization processes (Dessimoz et al., 2012; Chiaradia, 2009; Li J W et al., 2009; Richards and Kerrich, 2007; Macpherson et al., 2006); (3) partial melting of the lower continental crust in relation to delamination or crustal thickening (Yuan et al., 2010; Huang et al., 2008; Wang et al., 2007; Gao et al., 2004; Hou et al., 2004; Muir et al., 1995; Atherton and Petford, 1993; Kay and Kay, 1993). Previous studies suggested that the Qinling Orogen experienced a number of continent-continent collision events from the Middle Paleozoic to the Late Triassic, which was accomplished at 220–240 Ma due to a collision between the SCB and NCC (Wu et al., 2013a; Zhao et al., 2013; Dong et al., 2011; Meng and Zhang, 2000, 1999; Zhang et al., 1997, 1996; Li S G et al., 1993). However, as the formation of the Houyaoyu granite porphyries is ca. 131 Ma, there is no relationship between their formation and the collision events for the Qinling Orogen. The generation of the Houyaoyu granite porphyries is therefore not associated with partial melting of oceanic slab in a subduction setting, and this is also supported by the lack of contemporaneous mafic rocks (e.g., basalts, lamprophyres, diabases, gabbros) in East Qinling. In addition, there is no positive correlation between the SiO_2 and Sr/Y and La/Yb ratios (Fig. 11), and the diagram of La-La/Sm (Fig. 10b) shows that the parental magma of the Houyaoyu granite porphyries was generated by a partial melting process. Therefore, the Houyaoyu granite porphyries could not have resulted from the fractional crystallization of basaltic magma (Wang et al., 2014). Generally, adakitic rocks formed by crustal delamination have high MgO ($Mg^{\#}$>50), Cr (>30 ppm), and Ni (>20 ppm) (Richards and Kerrich, 2007), thus the Houyaoyu granite porphyries were not formed by a delaminated lower continental crust. Furthermore, the Houyaoyu granite porphyries are characterized by depletion of HREEs, Y, and negative $\varepsilon_{Nd}(t)$ values (-9.13– -12.3), which could be well explained by the partial melting of an over-thickened lower continental crust (generally having a depth of >50 km, ~15 kbar) (Wang et al., 2014; Hou et al., 2013, 2004). Finally, the South China Block was fully connected to the North China Plate by the Late Triassic, implying that there is no direct relationship between the formation of these small intrusions and the closure of the North Qinling Ocean.

On the chondrite-normalized REE diagram (Fig. 7a), the Houyaoyu granite porphyries are characterized by no (or

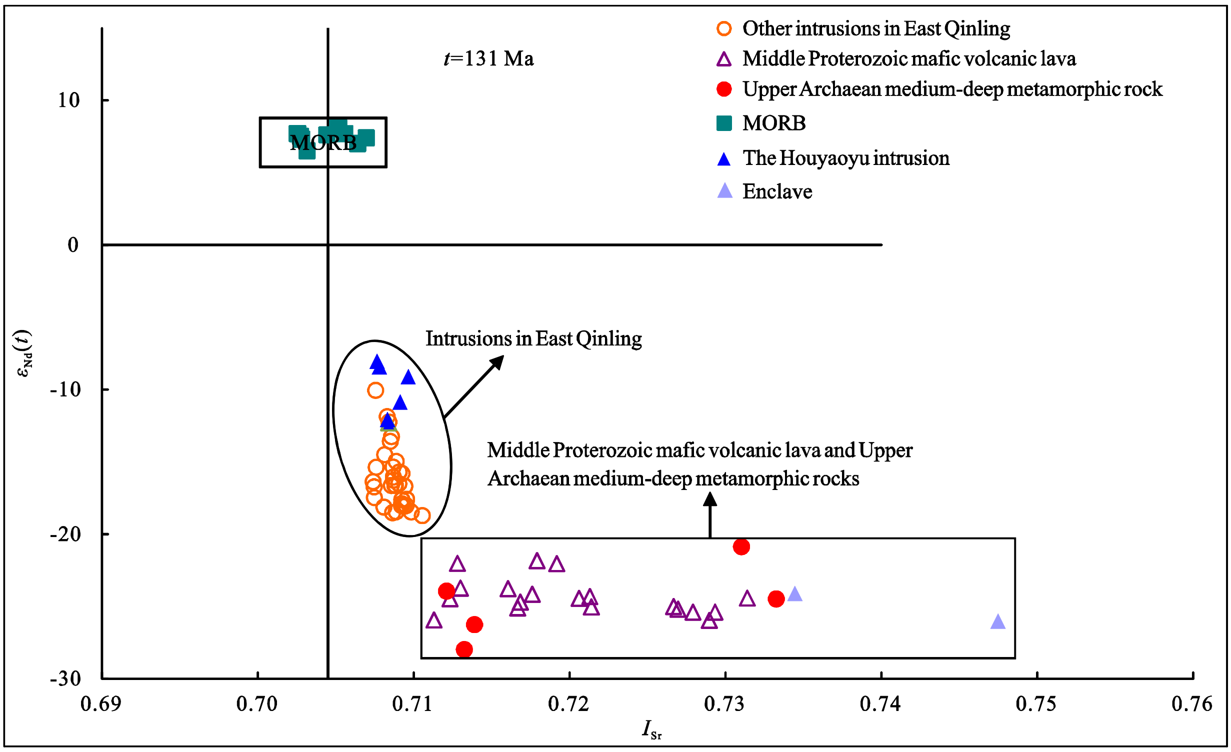

Figure 8. $\varepsilon_{Nd}(t)$ vs. I_{Sr} diagram of the Houyaoyu granite porphyries. Data of other intrusions in East Qinling include the Wenyu (Zhao et al., 2012), Niangniangshan (Zhao et al., 2012), Huashan (Ni et al., 2009), Laoniushan (Ni et al., 2009; Zhang et al., 2006), Heyu (Zhang et al., 2006), Lantian intrusions (Wang et al., 2011; Zhang et al., 2006), Xiong'er Group (Cui et al., 2011; He et al., 2010). The Taihua Group (Ni et al., 2009; Xu et al., 2009) is used to represent lower continental crust of the NCC, and MORB (Jacobsen and Wasserburg, 1979) is used to represent primitive mantle.

weakly negative) Eu anomalies, with δEu varying from 0.69 to 0.98, which suggests that almost no plagioclase fractionation occurred in the evolutional process of parental magma, or no plagioclase served as a residual component during intracrustal partial melting. In addition, high $(La/Yb)_N$ values indicate that parental magma experienced a long evolutionary time, or stand for the geochemical composition of the protolith. Figure 7b shows the negative anomalies for P, suggesting that apatite played an important role in crystal fractionation, and this is also evident from the negative correlation between P_2O_5 and SiO_2. Because there are no significant trends between TiO_2, Nb, Ta, and SiO_2, it is suggested that the negative anomalies for Nb, Ta, and Ti (Fig. 7b) are inherited from a crustal source, which is also supported by the strongly positive Pb anomalies.

The Sr-Nd isotopic compositions of the Houyaoyu granite porphyries are divided into two obvious groups (Table 3). One group with medium initial $^{87}Sr/^{86}Sr$ ratios (0.707 7–0.709 7) and negative $\varepsilon_{Nd}(t)$ values (-9.13– -12.3) represents the composition of the Houyaoyu granite porphyries and implies that they originated from the lower crust. However, the Sr-Nd isotopic characteristics are different from those of the lower crust of the NCC, indicating that mantle materials were involved in the generation of parental magma. The two enclave samples have high initial $^{87}Sr/^{86}Sr$ ratios (0.734 5 and 0.747 5) and more negative $\varepsilon_{Nd}(t)$ values (-24.26 and -26.04), similar to those of the ancient lower crust of the NCC.

We summarized Sr-Nd isotopic data for another six intrusions in East Qinling, and plotted their $\varepsilon_{Nd}(t)$ and initial $^{87}Sr/^{86}Sr$ ratios (I_{Sr}) values in Fig. 8. In the $\varepsilon_{Nd}(t)$ vs. I_{Sr} diagram, most of the data for the intrusions (except YY-22 and YY-56) in East Qinling are plotted in an area between MORB (representing primitive mantle) and the Xiong'er Group and Taihua Group (representing lower continental crust of NCC), suggesting a mixing source of mantle and crust. In addition, low MgO, Ni, and V concentrations also indicate the presence of minor mantle materials in the source. The ancient two-stage depleted- mantle Nd model ages (T_{2DM}) from 1.57 to 1.91 Ga, overlapping the ages of two inherited zircons in this study, suggest that the Houyaoyu granite porphyries might be derived from old lower continental crust.

In summary, we suggest that the Houyaoyu granite porphyries originated from a crust-mantle interaction, mainly in relation to an ancient continental crust, with minor involvement of mantle-derived components. This interpretation is also be supported by the discovery of enclaves from the lower crust and the old U-Pb zircon ages.

4.2 Timing and Tectonic Setting of Magmatic Events in East Qinling

Our SIMS zircon U-Pb dating results show that the Houyaoyu granite porphyries formed at about 131 Ma (in the Early Cretaceous stage in geologic time scale); the Early Cretaceous Age is consistent with previous results from LA-ICP-MS zircon U-Pb dating (Hu et al., 2010), indicating that Pb-Zn polymetallic mineralization began at that time. As the combining of the North China Craton (NCC) and the South China Block (SCB) was completed before 200 Ma (Li N et al., 2015a; Wu et al., 2013a; Zhao et al., 2013; Dong et al., 2012, 2011; Liu et al., 2011; Meng and Zhang, 2000, 1999; Zhang et al., 1997, 1996), the formation of the Houyaoyu granite porphyries, therefore, has no relationship with the collision of the Qinling Orogen. The Qinling Orogen was subsequently involved in a transition from compression to extension, which is evidenced by many Mesozoic extensional structures (including

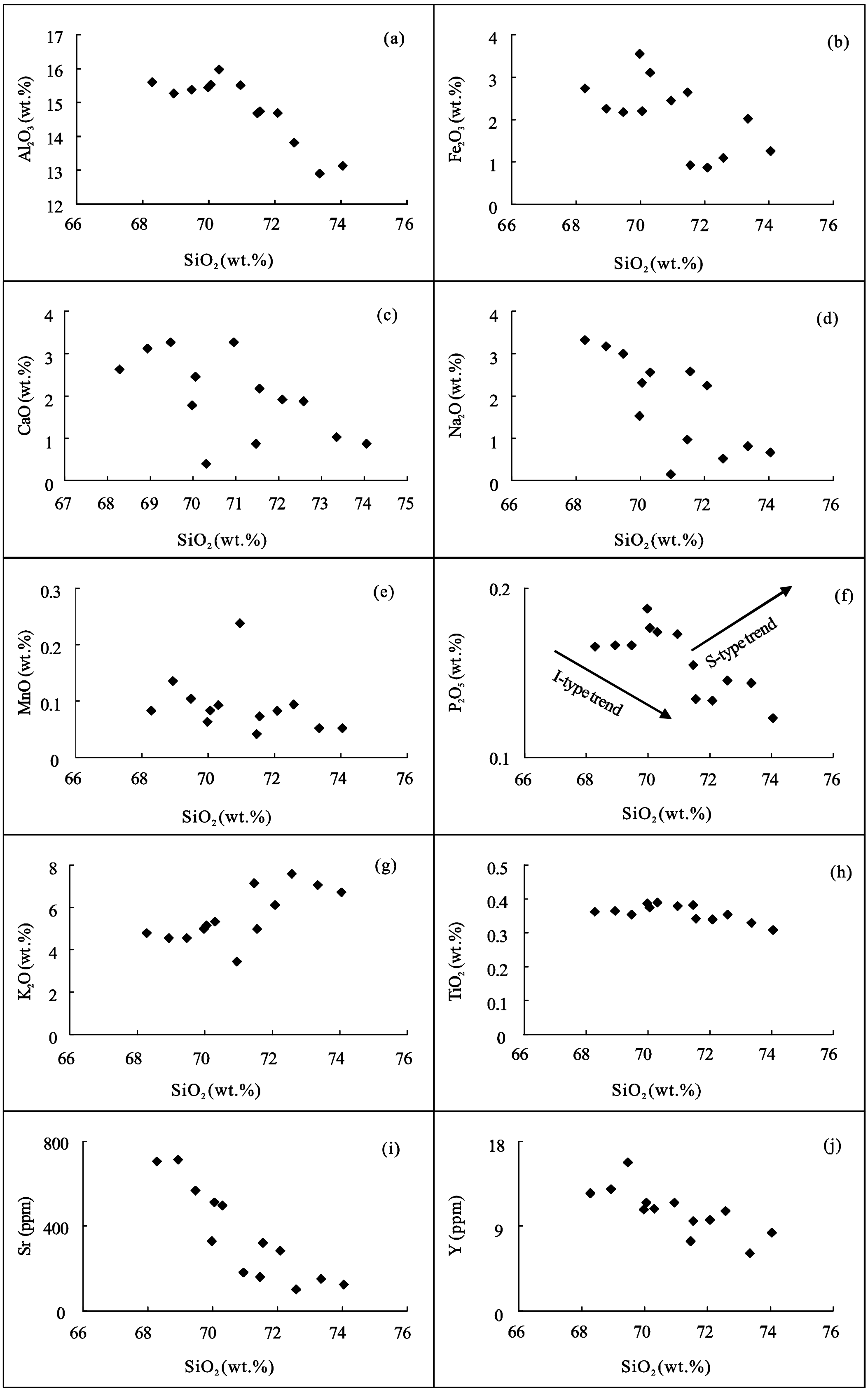

Figure 9. Major and trace elemental compositions versus SiO_2 diagrams.

metamorphic core complexes such as the Xiaoqinling, Xiaoshan, Xiong'ershan, and Lishan), and detachment faults developed during 135–123 Ma in the internal NCC (Lin et al., 2008; Yang et al., 2007; Liu et al., 2005; Zhang J J et al., 2003; Zhang and Li, 1998; Shi et al., 1993). In fact, the drifting Izanagi Plate turned to a roughly parallel direction to the Eurasian eastern continental margin after 135 Ma, rather than subducting beneath the continent (Goldfarb et al., 2007; Maruyama et al., 1997). This means that the Izanagi Plate had a reduced tectonic impact on the NCC after 135 Ma, and this is the main cause of the transition in the tectonic regime from compression to extension in the East Qinling district. Mantle materials began to upwell in an extensional tectonic environment and heated the over-thickened lower continental crust of the NCC, which led to partial melting of the crust. Lithospheric destruction of the North China Craton was simultaneously initiated; this caused numerous magmatic events that are confirmed by the large number of Mesozoic felsic intrusions in East Qinling.

On the basis of the above demonstration, we assumed that the Houyaoyu granite porphyries were formed in an extensional tectonic environment related to the lithospheric destruction of the North China Craton. The partial melting of the ancient lower continental crust of the NCC and the involvement of minor mantle materials generated the parental magma during mantle under plating, and crust-mantle interaction took place during the above processes. It is thus considered that Mo and Pb-Zn mineralization occurred in the Early Cretaceous in the south of NCC simultaneously with the destruction of the North China Craton (Bao et al., 2014; Mao et al., 2011).

4.3 Relationship between Magmatic Events with Mineralization in East Qinling

Numerous previous studies of the petrology, geochemistry,

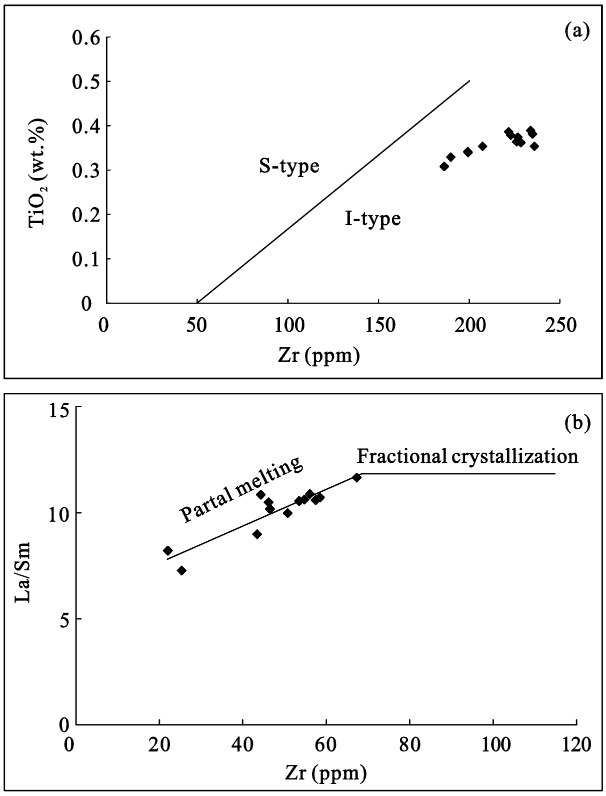

Figure 10. Plots of Zr versus TiO_2 and La versus La/Sm diagram of the Houyaoyu granite porphyries.

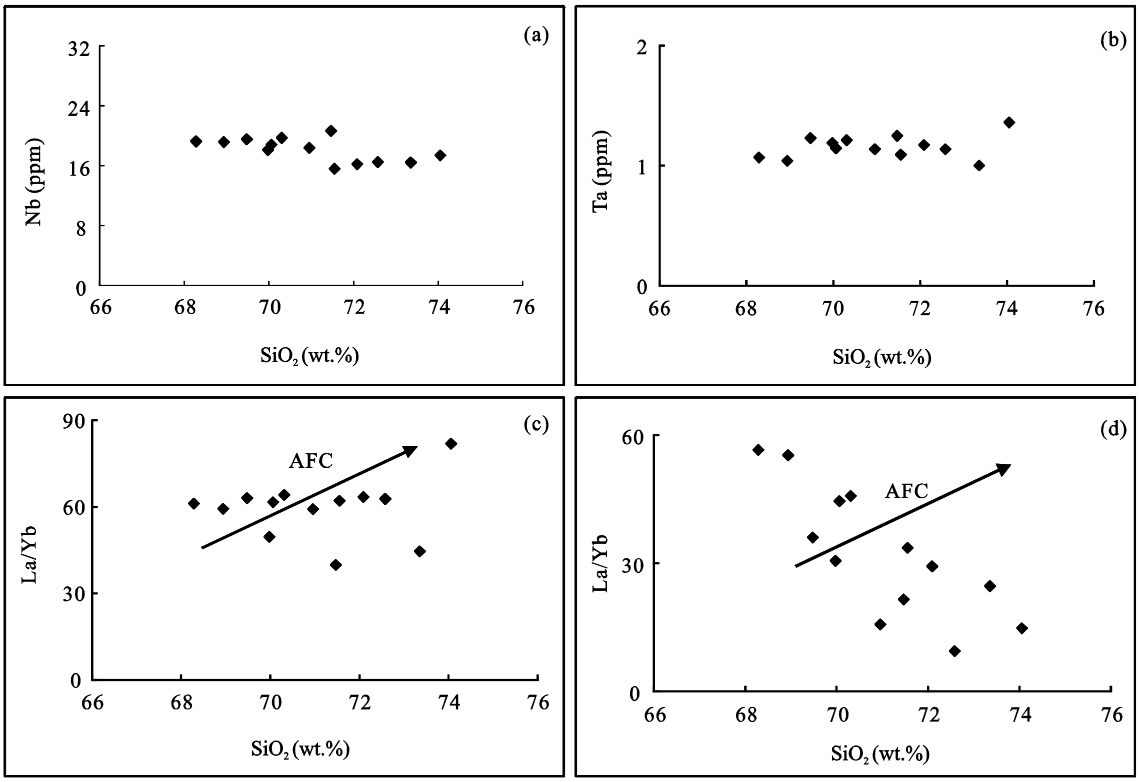

Figure 11. SiO_2 versus trace elements diagram of the Houyaoyu granite porphyries.

and geochronology for the Yanshanian intrusions in East Qinling have revealed two main magmatic events that occurred in the Late Jurassic–Early Cretaceous (158–141 Ma) and the Early Cretaceous (135–108 Ma), respectively (Li N et al., 2012; Qi et al., 2012; Hu et al., 2011; Wang et al., 2011; Gao et al., 2010; Mao et al., 2010; Dai et al., 2009; Guo et al., 2009; Ye et al., 2006; Zhang et al., 2006). The magmatism supplied such a large quantity of materials that formed a large-scale Mo mineralization belt and several Pb-Zn polymetallic deposits; all the Mo ore deposits and most of the Pb-Zn polymetallic deposits are related to the Yanshanian felsic intrusions. This proposal is also supported by the stable isotope characteristics (C, H, O, S) of vein minerals and Pb, Mo isotopes of ore minerals (Qi et al., 2012; Gao et al., 2010; Dai et al., 2009; Guo et al., 2009; Ye et al., 2006). The Houyaoyu intrusion is one of these intrusions in East Qinling, and it is closely related to the formation of Pb-Zn polymetallic deposits. Thus, its genesis is an important implication for the tectonic setting of the Early Cretaceous magmatic events and the relationship between magmatic events with mineralization in East Qinling District. Mao et al. (2011) summarized the characteristics and tectonic settings of Mesozoic molybdenum deposits in the East Qinling-Dabie orogenic belt, and found that these Mo deposits are genetically, spatially and temporally associated with Mesozoic intrusions. In fact, many vein type Pb-Zn-Ag deposits are located in the surrounding porphyry or porphyry-skarn Mo deposits, suggesting that they belong to the same ore system. Therefore, porphyry stock works and Pb-Zn polymetallic veins can be used as vectors for further prospecting in East Qinling Orogen.

5 CONCLUSIONS

(1) The Houyaoyu granite porphyries are I-type granites and have adakitic characteristics. The SIMS zircon U-Pb ages of the Houyaoyu granite porphyries are ~131 and ~133 Ma, suggesting that intense magmatic activities occurred during the Early Cretaceous in the south of the NCC.

(2) Trace elemental and Sr-Nd isotopic compositions indicate that the Houyaoyu granite porphyries were mainly derived from ancient lower continental crust, with minor involvement of mantle-derived components. The resultant crust-mantle interaction provided large amounts of ore-forming materials for Mo, Pb, and Zn mineralization in East Qinling.

(3) It is thus proposed that the Houyaoyu granite porphyries formed in an extensional tectonic setting related to the lithospheric destruction of the North China Craton.

ACKNOWLEDGMENTS

This research was jointly supported by the National Key R&D Program of China (No. 2016YFC0600405) and the National Natural Foundation of China (Nos. 41425011, 41262004). The authors are grateful to Dr. Aimin Fang and his colleagues from Lushi Mining Co., Ltd for providing invaluable assistance during our field investigation, and also grateful to two anonymous reviewers and Dr. Jianbo Chen, Dr. Min Tang for their constructive reviews, which considerably improved the paper. The final publication is available at Springer via https://doi.org/10.1007/s12583-018-0788-2

REFERENCES CITED

Atherton, M. P., Petford, N., 1993. Generation of Sodium-Rich Magmas from Newly Underplated Basaltic Crust. *Nature*, 362(6416): 144–146. https://doi.org/10.1038/362144a0

Bader, T., Franz, L., Ratschbacher, L., et al., 2013. The Heart of China Revisited: II Early Paleozoic (Ultra)High-Pressure and (Ultra)High-Temperature Metamorphic Qinling Orogenic Collage. *Tectonics*, 32(4): 922–947. https://doi.org/10.1002/tect.20056

Bao, Z. W., Wang, C. Y., Zhao, T. P., et al., 2014. Petrogenesis of the Mesozoic Granites and Mo Mineralization of the Luanchuan Ore Field in the East Qinling Mo Mineralization Belt, Central China. *Ore Geology Reviews*, 57: 132–153. https://doi.org/10.1016/j.oregeorev.2013.09.008

Barbarin, B., 1999. A Review of the Relationships between Granitoid Types, Their Origins and Their Geodynamic Environments. *Lithos*, 46(3): 605–626. https://doi.org/10.1016/s0024-4937(98)00085-1

Belousova, E. A., Griffin, W. L., O'Reilly, S. Y., et al., 2002. Igneous Zircon: Trace Element Composition as an Indicator of Source Rock Type. *Contributions to Mineralogy and Petrology*, 143(5): 602–622. https://doi.org/10.1007/s00410-002-0364-7

Black, L. P., Kamo, S. L., Allen, C. M., et al., 2004. Improved $^{206}Pb/^{238}U$ Microprobe Geochronology by the Monitoring of a Trace-Element-Related Matrix Effect; SHRIMP, ID-TIMS, ELA-ICP-MS and Oxygen Isotope Documentation for a Series of Zircon Standards. *Chemical Geology*, 205(1/2): 115–140. https://doi.org/10.1016/j.chemgeo.2004.01.003

Boynton, W. V., 1984. Geochemistry of the Rare Earth Elements: Meteorite Studies. In: Henderson, P., ed., Rare Earth Element Geochemistry. Elsevier, New York. 63–114

Castillo, P. R., 2012. Adakite Petrogenesis. *Lithos*, 134/135: 304–316. https://doi.org/10.1016/j.lithos.2011.09.013

Chappell, B. W., White, A. J. R., 1974. Two Contrasting Granite Types. *Pacific Geology*, 8: 173–174

Chappell, B. W., White, A. J. R., 1992. I- and S-Type Granites in the Lachlan Fold Belt. *Transactions of the Royal Society of Edinburgh*: *Earth Sciences*, 83(1/2): 1–26. https://doi.org/10.1017/s0263593300007720

Chen, Y. J., Li, C., Zhang, J., et al., 2000. Sr and O Isotopic Characteristics of Porphyries in the Qinling Molybdenum Deposit Belt and Their Implication to Genetic Mechanism and Type. *Science in China Series D*: *Earth Sciences*, 43(S1): 82–94. https://doi.org/10.1007/bf02911935

Chen, Y. J., Sui, Y. H., Pirajno, F., 2003. Exclusive Evidences for CMF Model and a Case of Orogenic Silver Deposits: Isotope Geochemistry of the Tieluping Silver Deposit, East Qinling Orogeny. *Acta Petrologica Sinica*, 19(3): 551–568 (in Chinese with English Abstract)

Chen, Y. J., Zhao, Y. C., 1997. Geochemical Characteristics and Evolution of REE in the Early Precambrian Sediments: Evidences from the Southern Margin of the North China Craton. *Episodes*, 20: 109–116

Chen, Y. W., Hu, R. Z., Bi, X. W., et al., 2018. Zircon U-Pb Ages and Sr-Nd-Hf Isotopic Characteristics of the Huichizi Granitic Complex in the North Qinling Orogenic Belt and Their Geological Significance. *Journal of Earth Science*. https://doi.org/10.1007/s12583-017-0906-6

Chiaradia, M., 2009. Adakite-Like Magmas from Fractional Crystallization and Melting-Assimilation of Mafic Lower Crust (Eocene Macuchi Arc, Western Cordillera, Ecuador). *Chemical Geology*, 265(3/4): 468–487. https://doi.org/10.1016/j.chemgeo.2009.05.014

Cui, M. L., Zhang, B. L., Zhang, L. C., 2011. U-Pb Dating of Baddeleyite and Zircon from the Shizhaigou Diorite in the Southern Margin of North China Craton: Constrains on the Timing and Tectonic Setting of the Paleoproterozoic Xiong'er Group. *Gondwana Research*, 20(1): 184–193. https://doi.org/10.1016/j.gr.2011.01.010

Dai, B. Z., Jiang, S. Y., Wang, X. L., 2009. Petrogenesis of the Granitic Porphyry Related to the Giant Molybdenum Deposit in Donggou, Henan Province, China: Constraints from Petrogeochemistry, Zircon U-Pb Chronology and Sr-Nd-Hf Isotopes. *Acta Petrologica Sinica*, 25: 2889–2901 (in Chinese with English Abstract)

Defant, M. J., Drummond, M. S., 1990. Derivation of some Modern Arc Magmas by Melting of Young Subducted Lithosphere. *Nature*, 347(6294): 662–665. https://doi.org/10.1038/347662a0

Deng, J. F., Mo, X. X., Zhao, H. L., et al., 2004. A New Model for the Dynamic Evolution of Chinese Lithosphere: 'Continental Roots-Plume Tectonics'. *Earth-Science Reviews*, 65(3/4): 223–275. https://doi.org/10.1016/j.earscirev.2003.08.001

Deng, J. F., Su, S. G., Niu, Y. L., et al., 2007. A Possible Model for the Lithospheric Thinning of North China Craton: Evidence from the Yanshanian (Jura-Cretaceous) Magmatism and Tectonism. *Lithos*, 96(1/2): 22–35. https://doi.org/10.1016/j.lithos.2006.09.009

DePaolo, D. J., Linn, A. M., Schubert, G., 1991. The Continental Crustal Age Distribution: Methods of Determining Mantle Separation Ages from Sm-Nd Isotopic Data and Application to the Southwestern United States. *Journal of Geophysical Research*, 96(B2): 2071–2088. https://doi.org/10.1029/90jb02219

Dessimoz, M., Müntener, O., Ulmer, P., 2012. A Case for Hornblende Dominated Fractionation of Arc Magmas: The Chelan Complex (Washington Cascades). *Contributions to Mineralogy and Petrology*, 163(4): 567–589. https://doi.org/10.1007/s00410-011-0685-5

Ding, L. X., Ma, C. Q., Li, J. W., et al., 2010. LA-ICPMS Zircon U-Pb Ages of the Lantian and Muhuguan Granitoid Plutons, Southern Margin of the North China Craton: Implications for Tectonic Setting. *Geochimica*, 39 (5): 401–413 (in Chinese with English Abstract)

Diwu, C. R., Sun, Y., Liu, X. M., Wang, H. L., 2007. Zircon U-Pb Ages and Hf Isotopes and Their Geological Significance of Yiyang TTG Gneisses from Henan Province, China. *Acta Petrologica Sinica*, 23: 253–262 (in Chinese with English Abstract)

Dong, Y. P., Zhang, G. W., Neubauer, F., et al., 2011. Tectonic Evolution of the Qinling Orogen, China: Review and Synthesis. *Journal of Asian Earth Sciences*, 41(3): 213–237. https://doi.org/10.1016/j.jseaes.2011.03.002

Dong, Y. P., Liu, X. M., Zhang, G. W., et al., 2012. Triassic Diorites and Granitoids in the Foping Area: Constraints on the Conversion from Subduction to Collision in the Qinling Orogen, China. *Journal of Asian Earth Sciences*, 47: 123–142. https://doi.org/10.1016/j.jseaes.2011.06.005

Dong, Y. P., Santosh, M., 2016. Tectonic Architecture and Multiple Orogeny of the Qinling Orogenic Belt, Central China. *Gondwana Research*, 29(1): 1–40. https://doi.org/10.13039/501100001809

Gao, S., Rudnick, R. L., Carlson, R. W., et al., 2002. Re–Os Evidence for Replacement of Ancient Mantle Lithosphere beneath the North China Craton. *Earth and Planetary Science Letters*, 198(3/4): 307–322. https://doi.org/10.1016/s0012-821x(02)00489-2

Gao, S., Rudnick, R. L., Yuan, H. L., et al., 2004. Recycling Lower Continental Crust in the North China Craton. *Nature*, 432(7019): 892–897. https://doi.org/10.1038/nature03162

Gao, X. Y., Zhao, T. P., Bao, Z. W., et al., 2014. Petrogenesis of the Early Cretaceous Intermediate and Felsic Intrusions at the Southern Margin of the North China Craton: Implications for Crust-Mantle Interaction. *Lithos*, 206/207: 65–78. https://doi.org/10.13039/501100001809

Gao, Y. L., Zhang, J. M., Ye, Y. S., et al., 2010. Geological Characteristics and Molybdenite Re-Os Isotopic Dating of Shiyaogou Porphyry Molybdenum Deposit in the East Qinling. *Acta Petrologica Sinica*, 26(3): 729–739 (in Chinese with English Abstract)

Ghosh, S. C., Nandi, A., Ahmed, G., et al., 1996. Study of Permo-Triassic Boundary in Gondwana Sequence of Raniganj Basin. In: Proceedings IXth international Gondwana Symposium. Oxford and IBH Publisher, New Delhi. 195–206

Goldfarb, R. J., Hart, C., Davis, G., et al., 2007. East Asian Gold: Deciphering the Anomaly of Phanerozoic Gold in Precambrian Cratons. *Economic Geology*, 102(3): 341–345. https://doi.org/10.2113/gsecongeo.102.3.341

Griffin, W. L., Zhang, A., O'Reilly, S. Y., et al., 1998. Phanerozoic Evolution of the Lithosphere beneath the Sino-Korean Craton. In: Flower, M. F., Chung, S. L., Lo, C. H., et al., eds., Mantle Dynamics and Plate Interaction in East Asia. American Geophysical Union Geodynamics Series 27, Washington, D.C.. 107–126

Guo, B., Zhu, L. M., Li, B., et al., 2009. Zircon U-Pb Age and Hf Isotope Composition of the Huashan and Heyu Granite Plutons at the Southern Margin of North China Craton: Implications for Geodynamic Setting. *Acta Petrologica Sinica*, 25: 265–281 (in Chinese with English Abstract)

Gutscher, M. A., Maury, R., Eissen, J. P., et al., 2000. Can Slab Melting be Caused by Flat Subduction?. *Geology*, 28(6): 535.

Hastie, A. R., Kerr, A. C., Pearce, J. A., et al., 2007. Classification of Altered Volcanic Island Arc Rocks Using Immobile Trace Elements: Development of the Th-Co Discrimination Diagram. *Journal of Petrology*, 48(12): 2341–2357. https://doi.org/10.1093/petrology/egm062

He, X. H., Zhong, H., Zhu, W. G., et al., 2014. Enrichment of Platinum-Group Elements (PGE) and Re-Os Isotopic Tracing for Porphyry Copper (Gold) Deposits. *Acta Geologica Sinica*: *English Edition*, 88(4): 1288–1309. https://doi.org/10.1111/1755-6724.12289

He, Y. H., Zhao, G. C., Sun, M., et al., 2010. Petrogenesis and Tectonic Setting of Volcanic Rocks in the Xiaoshan and Waifangshan Areas along the Southern Margin of the North China Craton: Constraints from Bulk-Rock Geochemistry and Sr-Nd Isotopic Composition. *Lithos*, 114(1/2): 186–199. https://doi.org/10.1016/j.lithos.2009.08.008

Hou, Z. Q., Gao, Y. F., Qu, X. M., et al., 2004. Origin of Adakitic Intrusives Generated during Mid-Miocene East-West Extension in Southern Tibet. *Earth and Planetary Science Letters*, 220(1/2): 139–155. https://doi.org/10.1016/s0012-821x(04)00007-x

Hou, Z. Q., Zheng, Y. C., Yang, Z. M., et al., 2013. Contribution of Mantle Components within Juvenile Lower-Crust to Collisional Zone Porphyry Cu Systems in Tibet. *Mineralium Deposita*, 48(2): 173–192. https://doi.org/10.1007/s00126-012-0415-6

Hu, H., Li, J. W., Deng, X. D., 2010. LA-ICP-MS Zircon U-Pb Dating of Granitoid Intrusions Related to Iron-Copper Polymetallic Deposits in Luonan-Lushi Area of Southern North China Craton and Its Geological Implications. *Mineral Deposits*, 30: 979–1001 (in Chinese with English Abstract)

Hu, S. X., Lin, Q. L., 1988. Geology and Mineralization in Convergence Belt between North China Craton and South China Block. Nanjing University Press, Nanjing. 1–277

Huang, F., Li, S. G., Dong, F., et al., 2008. High-Mg Adakitic Rocks in the Dabie Orogen, Central China: Implications for Foundering Mechanism of Lower Continental Crust. *Chemical Geology*, 255(1/2): 1–13. https://doi.org/10.1016/j.chemgeo.2008.02.014

Jacobsen, S. B., Wasserburg, G. J., 1979. Nd and Sr Isotopic Study of the Bay of Islands Ophiolite Complex and the Evolution of the Source of Midocean Ridge Basalts. *Journal of Geophysical Research*: *Solid Earth*, 84(B13): 7429–7445. https://doi.org/10.1029/jb084ib13p07429

Kay, R. W., Kay, S. M., 1993. Delamination and Delamination Magmatism. *Tectonophysics*, 219(1/2/3): 177–189. https://doi.org/10.1016/0040-1951(93)90295-u

Li, C. Y., Wang, F. Y., Hao, X. L., et al., 2012. Formation of the World's Largest Molybdenum Metallogenic Belt: A Plate-Tectonic Perspective on the Qinling Molybdenum Deposits. *International Geology Review*, 54(9): 1093–1112. https://doi.org/10.1080/00206814.2011.623039

Li, D., Zhang, S. T., Yan, C. H., et al., 2012. Late Mesozoic Time Constraints on Tectonic Changes of the Luanchuan Mo Belt, East Qinling Orogen, Central China. *Journal of Geodynamics*, 61: 94–104. https://doi.org/10.1016/j.jog.2012.02.005

Li, H. Y., Wang, X. X., Ye, H. S., et al., 2012. Emplacement Ages and Petrogenesis of the Molybdenum-Bearing Granites in the Jinduicheng Area of East Qinling, China: Constraints from Zircon U-Pb Ages and Hf Isotopes. *Acta Geologica Sinica - English Edition*, 86(3): 661–679. https://doi.org/10.1111/j.1755-6724.2012.00694.x

Li, J. W., Zhao, X. F., Zhou, M. F., et al., 2009. Late Mesozoic Magmatism from the Daye Region, Eastern China: U-Pb Ages, Petrogenesis, and Geodynamic Implications. *Contributions to Mineralogy and Petrology*, 157(3): 383–409. https://doi.org/10.1007/s00410-008-0341-x

Li, N., Chen, Y. J., Pirajno, F., et al., 2012. LA-ICP-MS Zircon U-Pb Dating, Trace Element and Hf Isotope Geochemistry of the Heyu Granite Batholith, Eastern Qinling, Central China: Implications for Mesozoic Tectono-Magmatic Evolution. *Lithos*, 142/143: 34–47. https://doi.org/10.1016/j.lithos.2012.02.013

Li, N., Chen, Y. J., Zhang, H., et al., 2007. Molybdenum Deposits in East Qinling. *Earth Science Frontiers*, 14: 186–198 (in Chinese with English Abstract)

Li, N., Chen, Y. J., Santosh, M., et al., 2015a. Compositional Polarity of Triassic Granitoids in the Qinling Orogen, China: Implication for Termination of the Northernmost Paleo-Tethys. *Gondwana Research*, 27(1): 244–257. https://doi.org/10.13039/501100001809

Li, N., Chen, Y. J., McNaughton, N. J., et al., 2015b. Formation and Tectonic Evolution of the Khondalite Series at the Southern Margin of the North China Craton: Geochronological Constraints from a 1.85-Ga Mo Deposit in the Xiong'ershan Area. *Precambrian Research*, 269: 1–17. https://doi.org/10.13039/501100001809

Li, Q. L., Li, X. H., Liu, Y., et al., 2010. Precise U-Pb and Pb-Pb Dating of Phanerozoic Baddeleyite by SIMS with Oxygen Flooding Technique. *Journal of Analytical Atomic Spectrometry*, 25(7): 1107. https://doi.org/10.1039/b923444f

Li, S. G., Xiao, Y. L., Liou, D. L., et al., 1993. Collision of the North China and Yangtse Blocks and Formation of Coesite-Bearing Eclogites: Timing and Processes. *Chemical Geology*, 109(1/2/3/4): 89–111. https://doi.org/10.1016/0009-2541(93)90063-o

Li, X. H., Liu, Y., Li, Q. L., et al., 2009. Precise Determination of Phanerozoic Zircon Pb/Pb Age by Multicollector SIMS without External Standardization. *Geochemistry*, *Geophysics*, *Geosystems*, 10(4): Q04010. https://doi.org/10.1029/2009gc002400

Li, Y. F., Mao, J. W., Guo, B. J., et al., 2004. Re-Os Dating of Molybdenite from the Nannihu Mo(-W) Orefield in the East Qinling and Its Geodynamic Significance. *Acta Geologica Sinica*: *English Edition*, 78(2): 463–470. https://doi.org/10.1111/j.1755-6724.2004.tb00155.x

Lin, W., Faure, M., Monié, P., et al., 2008. Mesozoic Extensional Tectonics in Eastern Asia: The South Liaodong Peninsula Metamorphic Core Complex (NE China). *The Journal of Geology*, 116(2): 134–154. https://doi.org/10.1086/527456

Liu, J. L., Davis, G. A., Lin, Z. Y., et al., 2005. The Liaonan Metamorphic Core Complex, Southeastern Liaoning Province, North China: A Likely Contributor to Cretaceous Rotation of Eastern Liaoning, Korea and Contiguous Areas. *Tectonophysics*, 407(1/2): 65–80. https://doi.org/10.1016/j.tecto.2005.07.001

Liu, S. W., Yang, P. T., Li, Q. G., et al., 2011. Indosinian Granitoids and Orogenic Processes in the Middle Segment of the Qinling Orogen: China. *Journal of Jilin University* (*Earth Science Edition*), 41: 1928–1943 (in Chinese with English Abstract)

Loiselle, M. C., Wones, D. R., 1979. Characteristics and Origin of Anorogenic Granites. *Geological Society of America Abstracts with Programs*, 11: 468

Lu, J. S., Wang, G. D., Wang, H., et al., 2015. Zircon SIMS U-Pb Geochronology of the Lushan Terrane: Dating Metamorphism of the Southwestern Terminal of the Palaeoproterozoic Trans-North China Orogen. *Geological Magazine*, 152(2): 367–377. https://doi.org/10.1017/s0016756814000430

Lu, X. X., 1998. Revealing the Process of Orogenic Evolution from Granites in the Qinling—Research Progress of the Qinling Granite. *Advances in Earth Sciences*, 13(2): 213–214 (in Chinese)

Ludwig, K. R., 2001. User-Manual for Isoplot/Ex Revsion 2.49. Berkeley Geochronology Centre, Special Publication, Berkeley. 4

Macpherson, C. G., Dreher, S. T., Thirlwall, M. F., 2006. Adakites without Slab Melting: High Pressure Differentiation of Island Arc Magma, Mindanao, the Philippines. *Earth and Planetary Science Letters*, 243(3/4): 581–593. https://doi.org/10.1016/j.epsl.2005.12.034

Mao, J. W., Pirajno, F., Xiang, J. F., et al., 2011. Mesozoic Molybdenum Deposits in the East Qinling–Dabie Orogenic Belt: Characteristics and Tectonic Settings. *Ore Geology Reviews*, 43(1): 264–293. https://doi.org/10.1016/j.oregeorev.2011.07.009

Mao, J. W., Xie, G. Q., Pirajno, F., et al., 2010. Late Jurassic-Early Cretaceous Granitoid Magmatism in Eastern Qinling, Central-Eastern China: SHRIMP Zircon U-Pb Ages and Tectonic Implications. *Australian Journal of Earth Sciences*, 57(1): 51–78. https://doi.org/10.1080/08120090903416203

Martin, H., Smithies, R. H., Rapp, R., et al., 2005. An Overview of Adakite, Tonalite-Trondhjemite-Granodiorite (TTG), and Sanukitoid: Relationships and Some Implications for Crustal Evolution. *Lithos*, 79(1/2): 1–24. https://doi.org/10.1016/j.lithos.2004.04.048

Maruyama, S., Isozaki, Y., Kimura, G., et al., 1997. Paleogeographic Maps of the Japanese Islands: Plate Tectonic Synthesis from 750 Ma to the Present. *The Island Arc*, 6(1): 121–142. https://doi.org/10.1111/j.1440-1738.1997.tb00043.x

Meng, Q. R., Zhang, G. W., 1999. Timing of Collision of the North and South China Blocks: Controversy and Reconciliation. *Geology*, 27(2): 123. https://doi.org/10.1130/0091-7613(1999)027<0123:tocotn>2.3.co;2

Meng, Q. R., Zhang, G. W., 2000. Geologic Framework and Tectonic Evolution of the Qinling Orogen, Central China. *Tectonophysics*, 323(3/4): 183–196. https://doi.org/10.1016/s0040-1951(00)00106-2

Menzies, M. A., Xu, Y. G., 1998. Geodynamics of the North Chinacraton. In: Flower, M. F., Chung, S. L., Lo, C. H., et al., eds., Mantle Dynamics and Plate Interaction in East Asia. American Geophysical Union Geodynamics Series 27, Washington, D.C.. 115–165

Middlemost, E. A. K., 1985. Magmas and Magmatic Rocks. Longman, London. 1–266

Middlemost, E. A. K., 1994. Naming Materials in the Magma/igneous Rock System. *Earth-Science Reviews*, 37(3/4): 215–224. https://doi.org/10.1016/0012-8252(94)90029-9

Muir, R. J., Weaver, S. D., Bradshaw, J. D., et al., 1995. The Cretaceous Separation Point Batholith, New Zealand: Granitoid Magmas Formed by Melting of Mafic Lithosphere. *Journal of the Geological Society*, 152(4): 689–701. https://doi.org/10.1144/gsjgs.152.4.0689

Ni, Z. Y., Zhang, H., Xue, L. W., 2009. Pb-Sr-Nd Isotope Constraints on the Source of Ore-Forming Elements of the Dahu Au-Mo Deposit, Henan Province. *Acta Petrologica Sinica*, 25(11): 2823–2832 (in Chinese with English Abstract)

Peccerillo, A., Taylor, S. R., 1976. Geochemistry of Eocene Calc-Alkaline Volcanic Rocks from the Kastamonu Area, Northern Turkey. *Contributions to Mineralogy and Petrology*, 58(1): 63–81. https://doi.org/10.1007/bf00384745

Qi, L., Hu, J., Gregoire, D. C., 2000. Determination of Trace Elements in Granites by Inductively Coupled Plasma Mass Spectrometry. *Talanta*, 51(3): 507–513. https://doi.org/10.1016/s0039-9140(99)00318-5

Qi, Q. J., Wang, X. X., Ke, C. H., et al., 2012. Geochronology and Origin of the Laoniushan Complex in the Southern Margin of North China Craton and Their Implications: New Evidences from Zircon Dating, Hf Isotopes and Geochemistry. *Acta Petrologica Sinica*, 28: 279–301 (in Chinese with English Abstract)

Richards, J. P., Kerrich, R., 2007. Special Paper: Adakite-Like Rocks: Their Diverse Origins and Questionable Role in Metallogenesis. *Economic Geology*, 102(4): 537–576. https://doi.org/10.2113/gsecongeo.102.4.537

Shi, Q. Z., Qin, G. Q., Li, M. L., et al., 1993. Detachment Extensional Structure and Gold Mineralization of the Post-Orogenic Stage in the West Henan Province. *Henan Geology*, 11: 27–36 (in Chinese with English Abstract)

Sláma, J., Košler, J., Condon, D. J., et al., 2008. Plešovice Zircon—A New Natural Reference Material for U-Pb and Hf Isotopic Microanalysis. *Chemical Geology*, 249(1/2): 1–35. https://doi.org/10.1016/j.chemgeo.2007.11.005

Stacey, J. S., Kramers, J. D., 1975. Approximation of Terrestrial Lead Isotope Evolution by a Two-Stage Model. *Earth and Planetary Science Letters*, 26(2): 207–221. https://doi.org/10.1016/0012-821x(75)90088-6

Sun, S. S., McDonough, W. F., 1989. Chemical and Isotopic Systematics of Oceanic Basalts: Implications for Mantle Composition and Processes. *Geological Society*, *London*, *Special Publications*, 42(1): 313–345. https://doi.org/10.1144/gsl.sp.1989.042.01.19

Wang, J. P., Liu, Z. J., Liu, J. J., et al., 2018. Trace Element Compositions of Pyrite from the Shuangwang Gold Breccias, Western Qinling Orogen, China: Implications for Deep Ore Prediction. *Journal of Earth Science*, 29(3): 564–572. https://doi.org/10.1007/s12583-017-0751-7

Wang, Q., Wyman, D. A., Xu, J. F., et al., 2007. Early Cretaceous Adakitic Granites in the Northern Dabie Complex, Central China: Implications for Partial Melting and Delamination of Thickened Lower Crust. *Geochimica et Cosmochimica Acta*, 71(10): 2609–2636. https://doi.org/10.1016/j.gca.2007.03.008

Wang, X. S., Hu, R. Z., Bi, X. W., et al., 2014. Petrogenesis of Late Cretaceous I-Type Granites in the Southern Yidun Terrane: New Constraints on the Late Mesozoic Tectonic Evolution of the Eastern Tibetan Plateau. *Lithos*, 208/209: 202–219. https://doi.org/10.13039/501100005231

Wang, X. X., Wang, T., Qi, Q. J., et al., 2011. Temporal-Spatial Variations, Origin and Their Tectonic Significance of the Late Mesozoic Granites in the Qinling, Central China. *Acta Petrologica Sinica*, 27(6): 1573–1593 (in Chinese with English Abstract)

Wiedenbeck, M., Allé, P., Corfu, F., et al., 1995. Three Natural Zircon Standards for U-Th-Pb, Lu-Hf, Trace Element and REE Analyses. *Geostandards and Geoanalytical Research*, 19(1): 1–23. https://doi.org/10.1111/j.1751-908x.1995.tb00147.x

Wu, F. Y., Lin, J. Q., Wilde, S. A., et al., 2005. Nature and Significance of the Early Cretaceous Giant Igneous Event in Eastern China. *Earth and Planetary Science Letters*, 233(1/2): 103–119. https://doi.org/10.1016/j.epsl.2005.02.019

Wu, Y. B., Zheng, Y. F., 2004. Genesis of Zircon and its Constraints on Interpretation of U-Pb Age. *Chinese Science Bulletin*, 49(15): 1554–1569. https://doi.org/10.1007/bf03184122

Wu, Y. B., Zheng, Y. F., 2013a. Southward Accretion of the North China Block and the Tectonic Evolution of the Qinling-Tongbai-Hong'an Orogenic Belt. *Chinese Science Bulletin*, 58: 2246–2250

Wu, Y. B., Zheng, Y. F., 2013b. Tectonic Evolution of a Composite Collision Orogen: An Overview on the Qinling-Tongbai-Hong'an-Dabie-Sulu Orogenic Belt in Central China. *Gondwana Research*, 23(4): 1402–1428. https://doi.org/10.13039/501100002855

Xiao, E., Hu, J., Zhang, Z. Z., et al., 2012. Petrogeochemistry, Zircon U-Pb Dating and Lu-Hf Isotopic Compositions of the Haoping and Jinshanmiao Granites from the Huashan Complex Batholith in Eastern Qinling Orogen. *Acta Petrologica Sinica*, 25: 4031–4046 (in Chinese with English Abstract)

Xu, H. J., Zhang, J. F., 2018. Zircon Geochronological Evidence for Participation of the North China Craton in the Protolith of Migmatite of the North Dabie Terrane. *Journal of Earth Science*, 29(1): 30–42. https://doi.org/10.1007/s12583-017-0805-x

Xu, W. L., Wang, F., Pei, F. P., et al., 2013. Mesozoic Tectonic Regimes and Regional Ore-Forming Background in NE China: Constraints from Spatial and Temporal Variations of Mesozoic Volcanic Rock Associations. *Acta Petrologica Sinica*, 29(2): 339–353 (in Chinese with English Abstract)

Xu, X. S., Griffin, W. L., Ma, X., et al., 2009. The Taihua Group on the Southern Margin of the North China Craton: Further Insights from U-Pb Ages and Hf Isotope Compositions of Zircons. *Mineralogy and Petrology*, 97(1/2): 43–59. https://doi.org/10.1007/s00710-009-0062-5

Yang, J. H., Wu, F. Y., Chung, S. L., et al., 2007. Rapid Exhumation and Cooling of the Liaonan Metamorphic Core Complex: Inferences from $^{40}Ar/^{39}Ar$ Thermochronology and Implications for Late Mesozoic Extension in the Eastern North China Craton. *Geological Society of America Bulletin*, 119(11/12): 1405–1414. https://doi.org/10.1130/b26085.1

Ye, H. S., Mao, J. W., Li, Y. F., et al., 2008a. SHRIMP Zircon U-Pb and Molybdenite Re-Os Datings of the Superlarge Donggou Porphyry Molybdenum Deposit in the East Qinling, China, and Its Geological Implications. *Acta Geologica Sinica*: *English Edition*, 82(1): 134–145. https://doi.org/10.1111/j.1755-6724.2008.tb00332.x

Ye, H. S., Mao, J. W., Xu, L. G., et al., 2008b. SHRIMP Zircon U-Pb Dating and Geochemistry of the Taishanmiao Aluminous A-type Granite in Western Henan Province. *Geological Review*, 54: 699–711 (in Chinese with English Abstract)

Ye, H. S., Mao, J. W., Li, Y. F., et al., 2006. Characteristics and Metallogenic Mechanism of Mo-W and Pb-Zn-Ag Deposits in Nannihu Orefield, Western Henan Province. *Geoscience*, 20: 165–174 (in Chinese with English Abstract)

Yogodzinski, G. M., Kelemen, P. B., 1998. Slab Melting in the Aleutians: Implications of an Ion Probe Study of Clinopyroxene in Primitive Adakite and Basalt. *Earth and Planetary Science Letters*, 158(1/2): 53–65. https://doi.org/10.1016/s0012-821x(98)00041-7

Yuan, C., Zhou, M. F., Sun, M., et al., 2010. Triassic Granitoids in the Eastern Songpan Ganzi Fold Belt, SW China: Magmatic Response to Geodynamics of the Deep Lithosphere. *Earth and Planetary Science Letters*, 290(3/4): 481–492. https://doi.org/10.1016/j.epsl.2010.01.005

Zeng, L. J., Zhou, D., Xing, Y. C., et al., 2013a. Geochemistry and Petrogenesis of the Babaoshan Granite Porphyry in Lushi County, Henan Province. *Geochimica*, 42: 242–261 (in Chinese with English Abstract)

Zeng, L. J., Xing, Y. C., Zhou, D., et al., 2013b. LA-ICP-MS Zircon U-Pb Age and Hf Isotope Composition of the Babaoshan Granite Porphyries in Lushi County, Henan Province. *Geotectonica et Metallogenia*, 37(1): 65–77 (in Chinese with English Abstract)

Zhai, M. G., Zhu, R. X., Liu, J. M., et al., 2003. Key Timing of Mesozoic Tectonic Regime Transform in Eastern North China. *Science in China* (*Ser. D*), 33(10): 913–920 (in Chinese with English Abstract)

Zhai, M. G., Meng, Q. R., Liu, J. M., et al., 2004. Geological features of Mesozoic Tectonic Regime Inversion in Eastern North China and Implication for Geodynamics. *Earth Science Frontiers*, 11(3): 285–298 (in Chinese with English Abstract)

Zhai, M. G., 2004. Adakite and Related Granitoids from Partial Melting of Continental Lower Crust. *Acta Petrologica Sinica*, 20(2): 193–194

Zhang, G. W., Dong, Y. P., Yao, A. P., 1997. The Crustal Compositions, Structures and Tectonic Evolution of the Qinling Orogenic Belt. *Geology of Shanxi*, 15: 1–14 (in Chinese with English Abstract)

Zhang, G. W., Meng, Q. R., Yu, Z. P., et al., 1996. Orogenesis and Dynamics of the Qinling Orogen. *Chinese Science Bulletin*, 39: 225–234

Zhang, G. W., Zhang, B. R., Yuan, X. C., et al., 2001. Qinling Orogenic Belt and Continental Dynamics. Science Press, Beijing (in Chinese)

Zhang, Z. Q., Li, S. M., 1998. Sm-Nd, Rb-Sr Age and Its Geological Significance of Archean Taihua Group in Xiongershan, West Henan Province, Contributions of Early Precambrian Geology in North China Craton. Geological Publishing House, Beiijng. 123–132 (in Chinese with English Abstract)

Zhang, Z. Q., Zhang, G. W., Liu, D. Y., et al., 2006. Chronology and Geochemistry of Ophiolite, Granite, and Clastic Sedimentary Rocks in Qinling Orogen. Geological Press, Beijing (in Chinese)

Zhang, J. J., Zheng, Y. D., Liu, S. W., 2003. Mesozoic Tectonic Evolution and Ore-Deposits Formation in the Gold Mine Field of Xiaoqinling. *Chinese Journal of Geology*, 38(1): 74–84 (in Chinese with English Abstract)

Zhang, Z. W., Yang, X. Y., Dong, Y., et al., 2011. Molybdenum Deposits in the Eastern Qinling, Central China: Constraints on the Geodynamics. *International Geology Review*, 53(2): 261–290. https://doi.org/10.1080/00206810903053902

Zhang, Z. W., Zhang, Z. S., Dong, Y., et al., 2007. Molybdenum Deposits in Eastern Qinling, Central China: Deep Structural Constraints on Their Reformation. *Acta Mineralogical Sinica*, 27: 372–378 (in Chinese with English Abstract)

Zhang, Z. W., Zhu, B. Q., Chang, X. Y., et al., 2001. Petrogenetic-Metallogenetic Background and Time-Space Relationship of the East Qinling Molybdenum Ore Belt, China. *Geological Journal of China Universities*, 7: 307–315 (in Chinese with English Abstract)

Zhao, H. X., Jiang, S. Y., Frimmel, H. E., et al., 2012. Geochemistry, Geochronology and Sr-Nd-Hf Isotopes of Two Mesozoic Granitoids in the Xiaoqinling Gold District: Implication for Large-Scale Lithospheric Thinning in the North China Craton. *Chemical Geology*, 294/295: 173–189. https://doi.org/10.1016/j.chemgeo.2011.11.030

Zhao, Z. F., Zheng, Y. F., Dai, L. Q., 2013. Origin of Residual Zircon and the Nature of Magma Source for Post Collisional Granite in Continental Collision Zone. *Chinese Science Bulletin*, 58: 2285–2289